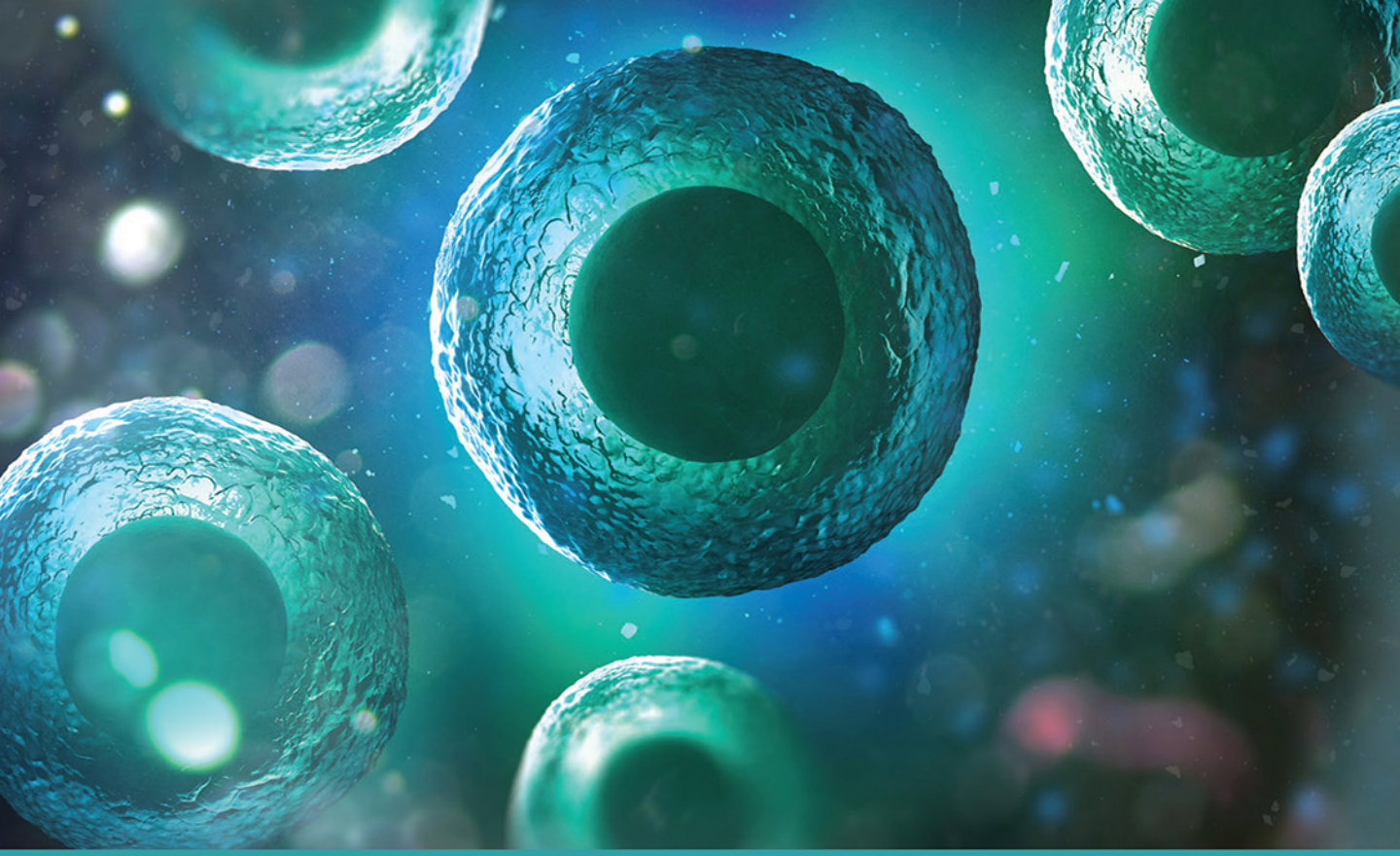

ADVANCES AND AVENUES IN THE DEVELOPMENT OF NOVEL CARRIERS FOR BIOACTIVES AND BIOLOGICAL AGENTS

EDITED BY
MANJU RAWAT SINGH
DEEPENDRA SINGH
JAGAT R. KANWAR
NAGENDRA SINGH CHAUHAN

ADVANCES AND AVENUES IN THE DEVELOPMENT OF NOVEL CARRIERS FOR BIOACTIVES AND BIOLOGICAL AGENTS

This page intentionally left blank

ADVANCES AND AVENUES IN THE DEVELOPMENT OF NOVEL CARRIERS FOR BIOACTIVES AND BIOLOGICAL AGENTS

Edited by

MANJU RAWAT SINGH
University Institute of Pharmacy, Pt. Ravishankar Shukla University, Raipur, India

DEEPENDRA SINGH
University Institute of Pharmacy, Pt. Ravishankar Shukla University, Raipur, India

JAGAT R. KANWAR
Nanomedicine-Laboratory of Immunology and Molecular Biomedical Research (NLIMBR), School of Medicine, Faculty of Health, Centre for Molecular and Medical Research (C-MMR), Deakin University, Waurn Ponds, VIC, Australia

NAGENDRA SINGH CHAUHAN
Drugs Testing Laboratory Avam Anusandhan Kendra (State Government Lab of AYUSH), Raipur, India

ELSEVIER

ACADEMIC PRESS

An imprint of Elsevier

Academic Press is an imprint of Elsevier
125 London Wall, London EC2Y 5AS, United Kingdom
525 B Street, Suite 1650, San Diego, CA 92101, United States
50 Hampshire Street, 5th Floor, Cambridge, MA 02139, United States
The Boulevard, Langford Lane, Kidlington, Oxford OX5 1GB, United Kingdom

British Library Cataloguing-in-Publication Data
A catalogue record for this book is available from the British Library

Library of Congress Cataloging-in-Publication Data
A catalog record for this book is available from the Library of Congress

ISBN: 978-0-12-819666-3

For Information on all Academic Press publications
visit our website at https://www.elsevier.com/books-and-journals

Publisher: Andre Gerhard Wolff
Acquisitions Editor: Erin Hill Parks
Editorial Project Manager: Tracy Tufaga
Production Project Manager: Swapna Srinivasan
Cover Designer: Christian J. Bilbow

Typeset by MPS Limited, Chennai, India

Contents

List of Contributors

Mohammed Abdelfattah Abdelwadod National Cancer Institute, Cairo University, Fom El Khalig, Cairo, Egypt

Ayman Aboda Nanomedicine-Laboratory of Immunology and Molecular Biomedical Research (NLIMBR), iMPACT Institute (CMMR-iMPACT) Deakin University, Waurn Ponds, VIC, Australia

Mukta Agrawal Rungta College of Pharmaceutical Sciences and Research, Bhilai, Chhattisgarh, India

Virginia Aiassa Faculty of Chemical Sciences, National University of Cordoba and CONICET, Cordoba, Argentina

Ajazuddin Rungta College of Pharmaceutical Sciences and Research, Bhilai, Chhattisgarh, India

Amit Alexander Department of Pharmaceutics, National Institute of Pharmaceutical Education and Research (NIPER-Guwahati), Department of Pharmaceuticals, Ministry of Chemicals & Fertilizers, Govt. of India, NH 37, NITS Mirza, Guwahati, Assam, India

Cátia G. Alves CICS-UBI—Health Sciences Research Centre, University of Beira Interior, Covilhã, Portugal

Daria V. Andreeva Materials Science and Engineering Department, National University of Singapore, Singapore, Singapore

Iman Attia National Cancer Institute, Cairo University, Fom El Khalig, Cairo, Egypt

João Basso Faculty of Pharmacy, University of Coimbra, Azinhaga de Santa Comba, Coimbra, Portugal; Centre for Neurosciences and Cell Biology (CNC), University of Coimbra, Rua Larga, Faculty of Medicine, Coimbra, Portugal; Coimbra Chemistry Center, Department of Chemistry, University of Coimbra, Coimbra, Portugal

David Bodenstein University of Toronto, Toronto, ON, Canada

Francine Carla Cadoná Franciscan University, Santa Maria, Brazil; University of West of Santa Catarina, Joaçaba, Brazil

Manuela Calin Institute of Cellular Biology and Pathology "N. Simionescu" of Romanian Academy, Bucharest, Romania

Durgesh Nandini Chauhan Columbia Institute of Pharmacy, Raipur, India

Nagendra Singh Chauhan Drugs Testing Laboratory Avam Anusandhan Kendra, Raipur, India

Ilídio J. Correia CICS-UBI—Health Sciences Research Centre, University of Beira Interior, Covilhã, Portugal; CIEPQPF—Chemical Process Engineering and Forest Products Research Centre - Chemical Engineering Department, University of Coimbra, Coimbra, Portugal

Duarte de Melo-Diogo CICS-UBI—Health Sciences Research Centre, University of Beira Interior, Covilhã, Portugal

Hossam S. El-Sawy Department of Pharmaceutics and Pharmaceutical Technology, Faculty of Pharmacy, Egyptian Russian University, Badr City, Egypt

Khalid M. El-Say Department of Pharmaceutics, Faculty of Pharmacy, King Abdulaziz University, Jeddah, Saudi Arabia; Department of Pharmaceutics and Industrial Pharmacy, Faculty of Pharmacy, Al-Azhar University, Cairo, Egypt

Fernanda Reis Favarin Franciscan University, Santa Maria, Brazil

Elena-Valeria Fuior Institute of Cellular Biology and Pathology "N. Simionescu" of Romanian Academy, Bucharest, Romania

Ahmed Gad National Cancer Institute, Cairo University, Fom El Khalig, Cairo, Egypt

Claudia Garnero Faculty of Chemical Sciences, National University of Cordoba and CONICET, Cordoba, Argentina

Ramesh K. Goyal Department of Pharmaceutics, Delhi Pharmaceutical Sciences and Research University, New Delhi, India

Andreas M. Grabrucker Bioscience and Bioengineering Research (BioSciBer), Bernal Biomaterials, Bernal Institute, University of Limerick, Limerick, Ireland; Department of Biological Sciences, University of Limerick, Limerick, Ireland; Health Research Institute (HRI), University of Limerick, Limerick, Ireland

Mine Silindir Gunay Department of Radiopharmacy, Faculty of Pharmacy, Hacettepe University, Ankara, Turkey; Department of Radiopharmacy, Faculty of Pharmacy, İzmir Katip Celebi University, İzmir, Turkey

Madhu Gupta Department of Pharmaceutics, Delhi Pharmaceutical Sciences and Research University, New Delhi, India

Numpon Insin Chulalongkorn University, Bangkok, Thailand

Gunjan Jeswani Faculty of Pharmaceutical Sciences, Shri Shankaracharya Group of Institutions, SSTC, Bhilai, Chhattisgarh, India

Jagat R. Kanwar Nanomedicine-Laboratory of Immunology and Molecular Biomedical Research (NLIMBR), Centre for Molecular and Medical Research (C-MMR), Strategic Research Centre, School of Medicine, Faculty of Health, Deakin University, Waurn Ponds, VIC, Australia

Rupinder Kaur Kanwar Nanomedicine-Laboratory of Immunology and Molecular Biomedical Research (NLIMBR), iMPACT Institute (CMMR-iMPACT) Deakin University, Waurn Ponds, VIC, Australia

Merve Karpuz Department of Radiopharmacy, Faculty of Pharmacy, Hacettepe University, Ankara, Turkey; Department of Radiopharmacy, Faculty of Pharmacy, İzmir Katip Celebi University, İzmir, Turkey

Vijay Kumar Nano Biotech Lab, Department of Zoology, Kirori Mal College, University of Delhi, Delhi, India

Rita Lima-Sousa CICS-UBI—Health Sciences Research Centre, University of Beira Interior, Covilhã, Portugal

Marcela R. Longhi Faculty of Chemical Sciences, National University of Cordoba and CONICET, Cordoba, Argentina

Alencar Kolinski Machado Franciscan University, Santa Maria, Brazil

Mamdouh Mahmoud Mostafa National Cancer Institute, Cairo University, Fom El Khalig, Cairo, Egypt

Jake Mazur School of Medicine, Faculty of health, iMPACT Institute (CMMR-iMPACT), Deakin University, Geelong, VIC, Australia

Kieran D. McGourty Bioscience and Bioengineering Research (BioSciBer), Bernal Biomaterials, Bernal Institute, University of Limerick, Limerick, Ireland; Health Research Institute (HRI), University of Limerick, Limerick, Ireland; Department of Chemical Sciences, University of Limerick, Limerick, Ireland

Mohamed A. Megahed Department of Pharmaceutics and Pharmaceutical Technology, Faculty of Pharmacy, Egyptian Russian University, Badr City, Egypt

Maria Mendes Faculty of Pharmacy, University of Coimbra, Azinhaga de Santa Comba, Coimbra, Portugal; Centre for Neurosciences and Cell Biology (CNC), University of Coimbra, Rua Larga, Faculty of Medicine, Coimbra, Portugal; Coimbra Chemistry Center, Department of Chemistry, University of Coimbra, Coimbra, Portugal

Vijay Mishra School of Pharmaceutical Sciences, Lovely Professional University, Phagwara, India

Mahmoud Mohsen Faculty of Pharmacy, Cairo University, Cairo, Egypt

André F. Moreira CICS-UBI—Health Sciences Research Centre, University of Beira Interior, Covilhã, Portugal

John J.E. Mulvihill Bioscience and Bioengineering Research (BioSciBer), Bernal Biomaterials, Bernal Institute, University of Limerick, Limerick, Ireland; School of Engineering, University of Limerick, Limerick, Ireland; Health Research Institute (HRI), University of Limerick, Limerick, Ireland

Aline Ferreira Ourique Franciscan University, Santa Maria, Brazil

A. Yekta Ozer Department of Radiopharmacy, Faculty of Pharmacy, Hacettepe University, Ankara, Turkey; Department of Radiopharmacy, Faculty of Pharmacy, İzmir Katip Celebi University, İzmir, Turkey

Alberto Pais Coimbra Chemistry Center, Department of Chemistry, University of Coimbra, Coimbra, Portugal

Arun K. Parihar Drugs Testing Laboratory Avam Anusandhan Kendra (State Goverment Lab of AYUSH), Government Ayurvedic College, Raipur, India

Madhulika Pradhan Rungta College of Pharmaceutical Sciences and Research, Bhilai, India

Vineet Kumar Rai CSIR-Central Institute of Medicinal and Aromatic Plants, Lucknow, India

Carolina F. Rodrigues CICS-UBI—Health Sciences Research Centre, University of Beira Interior, Covilhã, Portugal

Aisling M. Ross Bioscience and Bioengineering Research (BioSciBer), Bernal Biomaterials, Bernal Institute, University of Limerick, Limerick, Ireland; School of Engineering, University of Limerick, Limerick, Ireland

Carina Rossoni University of West of Santa Catarina, Joaçaba, Brazil

Kislay Roy School of Medicine, Faculty of health, iMPACT Institute (CMMR-iMPACT), Deakin University, Geelong, VIC, Australia

Swarnlata Saraf University Institute of Pharmacy, Pt. Ravishankar Shukla University, Raipur, India

Gaurav K. Saraogi NMIMS, School of Pharmacy and Technology Management, Shirpur, India

Kamal Shah Institute of Pharmaceutical Research, GLA University, Chaumuha, Mathura, India
Vikas Sharma Shri Rawatpura Sarkar Institute of Pharmacy, Datia, India
Sarah Shigdar School of Medicine, Faculty of health, iMPACT Institute (CMMR-iMPACT), Deakin University, Geelong, VIC, Australia
Sabahuddin Siddique Patel College of Pharmacy, Madhyanchal Professional University, Bhopal, Madhya Pradesh, India
Jessica Silva Faculty of Pharmacy, University of Coimbra, Azinhaga de Santa Comba, Coimbra, Portugal; Centre for Neurosciences and Cell Biology (CNC), University of Coimbra, Rua Larga, Faculty of Medicine, Coimbra, Portugal
Deependra Singh University Institute of Pharmacy, Pt. Ravishankar Shukla University, Raipur, India
Manju Rawat Singh University Institute of Pharmacy, Pt. Ravishankar Shukla University, Raipur, India
João Sousa Faculty of Pharmacy, University of Coimbra, Azinhaga de Santa Comba, Coimbra, Portugal; Coimbra Chemistry Center, Department of Chemistry, University of Coimbra, Coimbra, Portugal
Nidhi Srivastava CSIR-Central Institute of Medicinal and Aromatic Plants, Lucknow, India
Saurabh Srivastava School of Medical and Allied Sciences, Galgotias University, Greater Noida, India
Shikha Srivastava School of Medical and Allied Sciences, Galgotias University, Greater Noida, India
Wafa Taha National Cancer Institute, Cairo University, Fom El Khalig, Cairo, Egypt
Babu L. Tekwani Department of Infectious Diseases, Division of Drug Discovery, Southern Research, Birmingham, AL, United States
Anita Kamra Verma Nano Biotech Lab, Department of Zoology, Kirori Mal College, University of Delhi, Delhi, India
Vinay Sagar Verma Faculty of Pharmaceutical Sciences, Shri Shankaracharya Group of Institutions, SSTC, Bhilai, Chhattisgarh, India
Carla Vitorino Faculty of Pharmacy, University of Coimbra, Azinhaga de Santa Comba, Coimbra, Portugal; Centre for Neurosciences and Cell Biology (CNC), University of Coimbra, Rua Larga, Faculty of Medicine, Coimbra, Portugal; Coimbra Chemistry Center, Department of Chemistry, University of Coimbra, Coimbra, Portugal
Krishna Yadav University Institute of Pharmacy, Pt. Ravishankar Shukla University, Raipur, India
Narayan Prasad Yadav CSIR-Central Institute of Medicinal and Aromatic Plants, Lucknow, India
Nishika Yadav School of Pharmaceutical Sciences, Lovely Professional University, Phagwara, India
Pooja Yadav Rungta College of Pharmaceutical Sciences and Research, Bhilai, Chhattisgarh, India

CHAPTER

10

Inorganic-based drug delivery systems for cancer therapy

Carolina F. Rodrigues[1,*], *Cátia G. Alves*[1,*], *Rita Lima-Sousa*[1,*], *André F. Moreira*[1], *Duarte de Melo-Diogo*[1] *and Ilídio J. Correia*[1,2]

[1]CICS-UBI—Health Sciences Research Centre, University of Beira Interior, Covilhã, Portugal
[2]CIEPQPF—Chemical Process Engineering and Forest Products Research Centre - Chemical Engineering Department, University of Coimbra, Coimbra, Portugal

Abbreviations list

Au	Gold
AuMSS	Gold core silica shell nanoparticles
CTAB	Hexadecyltrimethylammonium bromide
CT	Computed tomography
DOX	Doxorubicin
EPR	Enhanced permeability and retention
GFN	Graphene family nanomaterials
GO	Graphene oxide
MSNs	Mesoporous silica nanoparticles
MSS	Mesoporous silica shell
NIR	Near infrared
PEI	Polyethylenimine
PEG	Polyethylene glycol
POX	Polyoxazolines
RES	Reticuloendothelial system
rGO	Reduced graphene oxide
RBCs	Red blood cells
ROS	Reactive oxygen species
SPR	Surface plasmon resonance
TEOS	Tetraethyl orthosilicate

* These authors contributed equally to this chapter.

Advances in the Development of Novel Carriers for Bioactives and Biological Agents
DOI: https://doi.org/10.1016/B978-0-12-819666-3.00010-9

10.1 Introduction

Cancer is the second leading cause of death globally (Bray et al., 2018). The GLOBOCAN estimates that in 2018 have been diagnosed 18.1 million new cases of cancer and 9.6 million deaths occurred as a consequence of this disease (Bray et al., 2018). Cancer is characterized by an uncontrolled proliferation of cells in response to genetic and epigenetic changes (Choi and Lee, 2013). During this process, cells acquire replicative immortality by avoiding the action of growth suppressors and death (Hanahan and Weinberg, 2011). Moreover, cells also gain the capacity to induce angiogenesis and to migrate from the tumor site to adjacent tissues, originating metastasis (Guan, 2015).

Up to now, conventional cancer therapies include the surgical resection of the tumor (performed in the early stages of cancer), chemotherapy, and radiotherapy (Desantis et al., 2014). However, these therapies display a suboptimal efficacy, leading to the incomplete tumor eradication, and as a consequence induce severe side effects on patients (e.g., hair loss, nausea, pain, edema, anemia) (Verma et al., 2018). Furthermore, tumor irradiation and chemotherapy have been showing to prompt prometastatic effects (Vilalta et al., 2016; Wrighton, 2019). In addition, cancer cells can acquire resistance to radio and chemotherapy further hindering their therapeutic capacity (Lin et al., 2016; Barker et al., 2015).

Researchers have been exploring new forms of cancer treatment to address these limitations. In particular, the use of inorganic nanomaterials [e.g., gold (Au), silica, or graphene] for the delivery of therapeutic agents (e.g., drugs, genes, immunomodulators) to cancer cells (Bayda et al., 2018). These nanoparticles can be engineered to accumulate passively or actively at the tumor zone, thus improving the efficacy of the loaded cargo as well as reducing the associated side effects. Moreover, the therapeutic agents' solubility and stability-related issues can be addressed through their incorporation in nanoparticles. Additionally, the physical properties of some inorganic nanoparticles can enable their use in cancer photothermal therapy and imaging (De Melo-Diogo et al., 2017b; Cheng et al., 2014; Huang et al., 2011). Due to these properties, there is a vast number of inorganic nanoparticles currently being evaluated in clinical trials, while others have already been approved by the Food and Drug Administration or the European Medicines Agency for human use (Bayda et al., 2018).

In this chapter, the use of gold-, silica-, and graphene-based nanoparticles in cancer therapy and imaging is highlighted. Initially, a general overview on the use of nanoparticles in cancer-related applications is provided, with emphasis on the main factors affecting their biodistribution and tumor accumulation. Then, the use of silica- (Section 10.3), gold- (Section 10.4), and graphene (Section 10.5)-based nanoparticles in cancer therapy and imaging will be analyzed. In Section 10.6, the application of hybrid nanostructures of silica/gold, silica/graphene, and graphene/gold in cancer theragnostic is assessed. Finally, Section 10.7 depicts the challenges, opportunities, and outlook regarding the use of these inorganic nanomaterials in cancer therapy and imaging.

10.2 Inorganic nanoparticles in cancer therapy and imaging

Inorganic nanoparticles used in cancer therapy are generally administered through intravenous administration. Once in the blood circulation, nanoparticles must avoid the

interaction with proteins since it can change their physicochemical properties (e.g., size or charge) (Blanco et al., 2015). On the other hand, opsonins' adsorption on nanoparticles' surface can lead to their recognition by the reticuloendothelial system (RES) (Duan and Li, 2013). These two events can mediate nanoparticles' blood clearance or accumulation in off-target organs (liver and spleen).

Subsequently, nanoparticles may become accumulated passively in the tumor zone by taking advantage from the enhanced permeability and retention (EPR) effect (Hobbs et al., 1998). The tumor vasculature displays leaky cell−cell junctions with fenestrae' sizes ranging from 200 to 1200 nm, enabling the nanoparticles' extravasation from the vessels to the tumor zone. Furthermore, the impaired lymphatic drainage of the tumor zone promotes the retention of the nanoparticles in this zone (Hoshyar et al., 2016). Recently, it was uncovered that besides these static pores on the vasculature, dynamic, and short-lived eruptions may occur in the blood vessels of the tumor zone (Matsumoto et al., 2016). These temporary eruptions can increase the blood flow into the tumor interstitial space, promoting nanoparticles' tumor accumulation (Matsumoto et al., 2016). In this way, it is of utmost importance to produce nanoparticles that display long blood circulation time to maximize their ability to benefit from these effects. Additionally, the nanoparticles' surface can be modified with targeting ligands that bind to receptors overexpressed in newly formed vessels, thus enhancing their tumor accumulation (De Melo-Diogo et al., 2018b; Duan and Li, 2013).

After nanoparticles' tumor accumulation, they need to penetrate into the tumor mass to achieve cellular internalization (Zhang et al., 2019; Ernsting et al., 2013). The high interstitial pressure found within the tumor zone and tumors' dense extracellular matrix can hinder nanoparticles' ability to reach the center of the tumor (Zhang et al., 2019). Ultimately, nanoparticles will be internalized by the cancer cells mainly through endocytosis (Hoshyar et al., 2016; Foroozandeh and Aziz, 2018; Duan and Li, 2013). Furthermore, nanoparticles can also target receptors overexpressed by cancer cells' membrane to achieve a higher selectivity (Akhtar et al., 2014). Upon cellular internalization, nanoparticles should release their loaded cargo into the cytoplasm. In this regard, some inorganic nanoparticles can intrinsically respond to stimuli (e.g., light) or be tailored to have responsiveness (e.g., pH), thus mediating a tumor cell-confined and controlled release of the therapeutics (Mura et al., 2013).

The size, charge, and shape of the different inorganic nanoparticles can significantly impact on their interaction with the different biological components, thus dictating nanoparticles' fate (Blanco et al., 2015). Furthermore, nanoparticles' corona composition and the presence of targeting moieties also play a crucial role on their biodistribution and tumor-homing capacity.

In the next subsections, the fine-tuning of the inorganic nanoparticles' properties (size, charge, shape, corona, and targeting moieties) with the aim of improving their blood circulation time, accumulation and penetration into the tumor, as well as their cellular internalization by the cancer cells will be discussed (Fig. 10.1).

10.2.1 Size

The size of inorganic nanoparticles strongly affects their biodistribution. Nanoparticles with a diameter under 5−10 nm tend to be rapidly cleared from circulation through renal

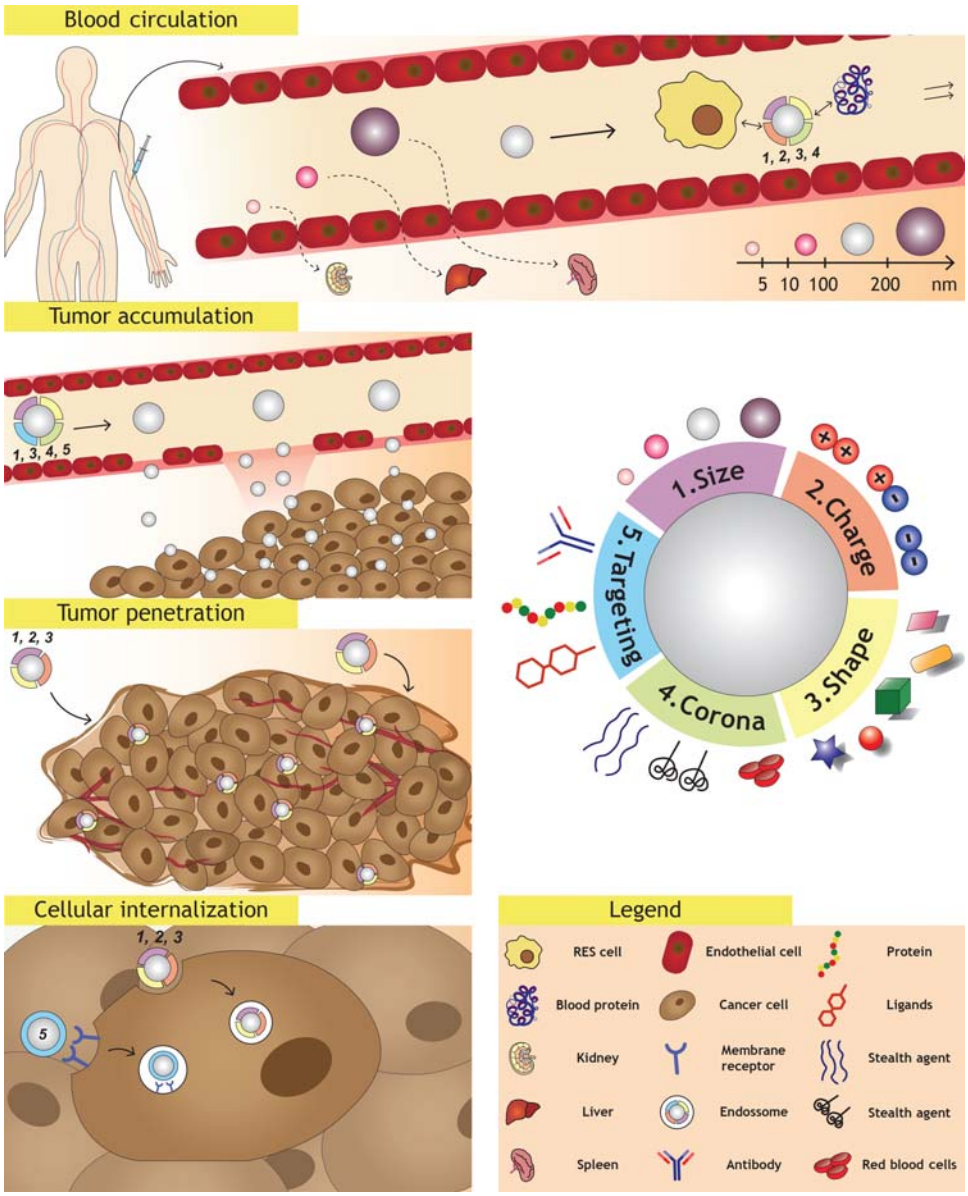

FIGURE 10.1 Schematic representation of the nanomaterials' properties that influence their blood circulation, tumor accumulation and penetration, as well as their uptake by cancer cells. These events are affected by different properties of the nanomaterials, represented using a color-coded scheme around the nanoparticle (purple: size; red: charge; yellow: shape; green: corona; and blue: targeting) and a number-coded scheme near the nanoparticle (1: 2: 3: 4: 5:).

filtration (Hoshyar et al., 2016; Blanco et al., 2015). Additionally, nanoparticles larger than 200 nm are prone to be recognized by macrophages or Kupffer cells, and to become accumulated in the RES organs (spleen and liver) (Hoshyar et al., 2016; Blanco et al., 2015). Moreover, nanomaterials smaller than 50 nm tend to accumulate in the liver by extravasation through its fenestrations (50−100 nm) (Hoshyar et al., 2016; Blanco et al., 2015). During nanoparticles' blood circulation, their opsonization by serum proteins can also modify their hydrodynamic diameter, thus impacting on nanoparticles' biodistribution (Blanco et al., 2015; Hoshyar et al., 2016).

Li et al. evaluated the biodistribution of Polyethylene glycol (PEG) functionalized gold nanoparticles with different sizes (6.2, 24.3, 42.5, and 61.2 nm) and as expected, the larger nanoparticles (42.5 and 61.2 nm) displayed an increased uptake by the liver (about 44%−55% ID/g) and spleen (about 30%−40% ID/g) after 24 h of administration (Li et al., 2018). In another work, Perrault et al. synthesized PEGylated gold nanoparticles with sizes of 20, 40, 60, 80, and 100 nm, and evaluated their blood circulation time (Perrault et al., 2009). The data obtained revealed that the 60 nm nanoparticles displayed the highest blood circulation half-time ($t_{1/2}$ of 16.5 h), followed by the 80 and 100 nm nanoparticles ($t_{1/2}$ of 11.5 and 7.2 h, respectively).

In this way, the size of inorganic nanoparticles strongly impacts on their ability to reach the tumor site. Considering the impact of the size on nanoparticles' clearance/accumulation in off-target organs and the features of the static and dynamic pores found in the tumor vasculature, it is often stated that the appropriate size range for nanoparticles' tumor accumulation is between 100 and 200 nm (Blanco et al., 2015). Nevertheless, the optimal size for each type of nanoformulation must be investigated since similar sized materials can display different tumor accumulation rates. In a recent study, 30 nm-sized PEGylated gold nanostars demonstrated a higher tumor uptake than their equivalents with 60 nm (2.11 ± 0.64 vs. 0.88 ± 0.46% ID/g) (Liu et al., 2015c). In another report, PEGylated gold nanoparticles with 60, 80, and 100 nm had the highest tumor accumulation (26.47%, 20.4%, and 17.0% ID/g over time, respectively) when compared with their 20 nm-sized equivalents (0.3% ID/g over time) (Perrault et al., 2009).

Furthermore, the size of the nanoparticle also plays an important role in their tumor penetration capacity (Zhang et al., 2019). Even though large nanoparticles can display a better tumor-homing capacity, these become mostly accumulated at the tumor periphery (Li et al., 2016). In contrast, small nanoparticles exhibit a better ability to penetrate the tumor mass (Li et al., 2016). For instance, 20 nm-sized PEGylated gold nanoparticles displayed a better diffusion in the tumor interstitial space when compared with their larger equivalents (60 and 100 nm) (Perrault et al., 2009). To develop a nanoformulation that displays a good tumor accumulation and penetration, Ruan et al. prepared gelatin nanoparticles incorporating PEGylated gold nanoparticles (Ruan et al., 2015). This hybrid nanoformulation displayed a size of 186.5 nm in conditions mimicking the blood circulation. In turn, the hybrids' size decreased to 59.3 nm upon treatment with metalloproteinase-2 (a tumor overexpressed enzyme that can cleave gelatin), rendering nanostructures with a size more favorable for tumor penetration.

Finally, nanoparticles' cellular internalization is also size dependent. Nanoparticles can interact with membrane receptors that mediate their internalization (Foroozandeh and Aziz, 2018; Saw et al., 2018; Blanco et al., 2015). In general, larger nanoparticles interact

more easily with these receptors, but they present a lower uptake rate. On the other hand, small nanoparticles can bypass the interaction with these receptors and diffuse directly to the cytoplasm (Foroozandeh and Aziz, 2018; Blanco et al., 2015).

10.2.2 Charge

The nanoparticles' surface charge is another important parameter with a huge impact on their blood circulation time, tumor penetration, and cellular internalization. In general, highly charged (positively or negatively) nanomaterials display a greater propensity to interact with the RES cells or to become opsonized (Xiao et al., 2011). Such events lead to nanoparticles blood clearance, thereby impairing their ability to reach the tumor site (Gessner et al., 2002). Moreover, highly charged nanomaterials display a low tumor penetration due to their interaction with the tumor's extracellular matrix components such as hyaluronic acid or collagen (Ernsting et al., 2013). Due to these events, the neutrally charged nanoparticles (zeta potential between −10 and +10 mV) are often considered ideal for cancer-related applications (De Melo-Diogo et al., 2017b).

On the other hand, positively charged nanomaterials can achieve a higher internalization in cancer cells by interacting with the negatively charged components of cells' membrane (e.g., phosphatidylserine and sialic acid). In this way, neutrally charged nanomaterials with a stimuli-responsive charge switch to positive values can display an augmented blood circulation time as well as display an enhanced cellular internalization. In this context, Wang et al. produced PEGylated gold nanostars with different contents of amine and carboxyl groups at their surface to modulate their charge in response to the extracellular environment pH (Wang et al., 2015b). Particularly, the nanostars with a ratio of four amines to one carboxyl group displayed a slightly negative surface charge (−14 mV) at physiological pH (7.4) and did become neutral (−6 mV) at the pH of the tumor microenvironment (6.4). Such charge-shift resulted in a lower uptake at pH 7.4 and higher uptake at pH 6.4 of the nanostars by cancer cells. In vivo, the charge-shift nanostars presented a high tumor accumulation of ≈ 10% ID/g, while their equivalents functionalized only with carboxyl (−27 mV) or amine groups (+13 mV) presented a tumor accumulation of ≈ 4% and 2% ID/g, respectively. In another report, Feng et al. functionalized PEGylated graphene oxide (GO) with poly(allylamine hydrochloride) modified with 2,3-dymethylmaleic anhydride to assemble a pH-dependent charge-switchable nanomaterial (Feng et al., 2014). At physiological pH, this nanoformulation displayed a surface charge of −12 mV. Whereas at the pH of the tumor microenvironment, the nanostructures became positively charged (+5 mV) due to the hydrolysis of the 2,3-dymethylmaleic anhydride groups. As importantly, this surface charge-shift to +5 mV greatly enhanced the uptake of this nanoformulation by cancer cells (Feng et al., 2014).

10.2.3 Shape

The nanoparticles' shape also plays a crucial role on its interaction with the human body. Nanoparticles' geometry (e.g., spheres, rods, cages, sheets) has been shown to influence their blood circulation time, cellular uptake, and in vivo fate. Nevertheless, the

contribution of the shape in these processes tends to be different for each type of nanoparticles (Huang et al., 2010; Black et al., 2014; Toy et al., 2014). In fact, the effect of shape in nanoparticles' capacity to reach the tumor zone has been subject of strong debate, and the results available in the literature are often inconsistent (Xie et al., 2017; Yue et al., 2017; Black et al., 2014). Moreover, the impact of nanocarriers' shape on cellular internalization needs to be further investigated.

During blood circulation, nanomaterials' shape mediates their interaction with macrophages. Black et al. demonstrated that gold nanospheres display a higher blood circulation time and lower RES uptake compared with gold nanorods, nanocages, and nanodisks (Black et al., 2014). Additionally, elongated particles exhibit orientation and aspect ratio–dependent internalization by macrophages (Champion and Mitragotri, 2006; Mitragotri et al., 2014).

Nanoparticles' shape also dictates the site of the blood vessels (periphery or central zone) where they circulate (Toy et al., 2014; Ta et al., 2018). Circulation near to the vessels' wall is required for nanoparticles to interact with the tumor vasculature and extravasate into the tumor site. This is desirable not only when the aim is to reach the tumor interstitium (cancer cells), but also when it is intended to target the tumor vessels. In opposition to the spherical nanoparticles that circulate in the center of the vessels, the rod-shaped nanoparticles undergo rotation and tumbling phenomena, which increases their lateral drift to the vessel walls, and consequently their probability to reach the tumor (Toy et al., 2014; Ta et al., 2018; Doshi et al., 2010). Janát-Amsbury and coworkers verified that PEGylated gold nanorods possess a higher tumor accumulation than PEGylated gold nanospheres, due to their longer circulation time and lower uptake by spleen and liver (Arnida et al., 2011).

In this way, the shape of the nanoparticles also influences their tumor uptake. For instance, gold nanospheres presented the highest tumor accumulation when compared with gold nanocages, nanodisks, and nanorods (Black et al., 2014). On the other hand, elongated-shaped materials presented an increased retention at the tumor site when compared with spherical nanoparticles (Black et al., 2014). In another study, PEGylated gold nanohexapods and nanorods presented a higher tumor-homing capacity (nanohexapods: $\approx$ 7.2% ID/g, gold nanorods: $\approx$ 8.4% ID/g) than PEGylated gold nanocages (2.6% ID/g) (Wang et al., 2013b).

In addition, the nanoparticle tumor penetration and distribution can also be affected by the shape. In this regard, nanocages and nanorods were mostly observed in the center of the tumors, while nanospheres and nanodisks are only found at the surface of the tumors (Black et al., 2014). On the other hand, Dias et al. demonstrated that silica–gold nanospheres display an increased penetration and distribution in 3D tumor spheroids when compared with nanorods (Dias et al., 2016).

The nanomaterials' geometry also affects their cellular uptake. For instance, increasing the aspect ratio of the gold nanorods can decrease their uptake by cells (Qiu et al., 2010). However, other studies reported that higher aspect ratios lead to a greater and faster cellular internalization (Huang et al., 2010). Dias et al. reported that gold nanorods functionalized with mesoporous silica shell (MSS) presented an increased cellular uptake when compared with spherical nanoparticles (Dias et al., 2016). On the other hand, the coating of palladium nanosheets with silica led to a conformation change of the nanoparticles,

from 2D to nanospheres (Tang et al., 2011). This shape conversion led to an ≈ 4.7-fold increase in the internalization by cancer cells. Additionally, Huang et al. studied the effect of mesoporous silica nanoparticles (MSNs) with different aspect ratios (1, 2, 4) in A375 cells internalization (Huang et al., 2010). The results suggest that larger nanoparticles (higher AR) present an increased and faster internalization. Nevertheless, it was also found that nanoparticles with higher AR, induced alterations in cell's functions, such as apoptosis, cytoskeleton formation, migration, and cell proliferation (Huang et al., 2010).

10.2.4 Corona

Nanoparticles' corona composition plays an important role in their interaction with biological components. Nanoparticles' surface can be functionalized with different compounds [e.g., hydrophilic polymers and red blood cells (RBCs) based coatings] to improve their solubility, stability, biodistribution, and biocompatibility (Ernsting et al., 2013; Gao et al., 2013; Lima-Sousa et al., 2018; Reis et al., 2019).

During blood circulation, some biological biomolecules (e.g., proteins) can adhere on nanoparticles' surface, forming a protein corona that affects nanoparticle's immunogenicity, cellular uptake, and pharmacokinetics (Lee et al., 2014; Walkey et al., 2012). Furthermore, the protein corona can also modify nanoparticles' size and charge as well as promote their aggregation. Such events can favor nanoparticles' elimination through the RES or change their safety profile (Kharazian et al., 2016; Bertrand et al., 2017; Walkey et al., 2012).

In this way, different strategies have been explored to functionalize the nanoparticles' surface to decrease the proteins adhesion as well as increase their blood circulation time and tumor accumulation. PEG, a hydrophilic and nontoxic polymer, is the most commonly used for this purpose (Otsuka et al., 2012; Kolate et al., 2014). PEG coatings are known to increase the nanomaterials' hydrophilicity and biocompatibility (Otsuka et al., 2012; Knop et al., 2010; Kolate et al., 2014). Furthermore, PEG creates a steric and hydration barrier around the surface of the nanoparticles that reduce protein adsorption and nanomaterials' uptake by the RES, leading to an increased blood circulation time and tumor uptake (Kolate et al., 2014; Pozzi et al., 2014). For example, the PEGylation of rod-shaped gold core silica shell nanoparticles (AuMSS) increased the nanomaterials' blood circulation time and their tumor uptake from 0.61 to 0.83% ID/g, when compared with the bovine serum albumin-coated counterparts (Wang et al., 2015a).

Still, the PEGylation' advantages are dependent on the PEG density, molecular weight, and grafting degree (Liu et al., 2015a; Uz et al., 2016). Liu et al. evaluated the impact of the PEG molecular weight (0.55, 1, 2, and 5 kDa) on the performance of PEGylated nanoparticles. Their results showed that the increase of the PEG molecular weight improved nanoparticles' cytocompatibility; however, those nanoparticles functionalized with the lowest molecular weight PEGs (0.55 and 1 kDa) demonstrated the highest cellular uptake, which emphasizes the importance of optimizing the PEG corona for an improved biological performance (Liu et al., 2015a).

Currently, different PEG-modified nanoparticles are used as anticancer therapies in the clinic (e.g., Doxil, GenexolPM, and DaunoXome). Despite their potential, PEG-coated nanomaterials have recently shown to be immunogenic (Wan et al., 2017). In fact, anti-PEG antibodies

can be created at the time of the injection of PEGylated nanomaterials, which subsequently accelerates their elimination at the time of the subsequent injections (Abu Lila et al., 2013; Ishida et al., 2003). This phenomenon is known as the accelerated blood clearance and motivated the investigation of PEG-alternatives to functionalize the nanomaterials' surface.

Polyoxazolines (POx), poly(glycerol), and poly(L-glutamic acid) are currently being investigated as PEG-alternatives (De Melo-Diogo et al., 2018a; Moreira et al., 2018b; Tukappa et al., 2016; Silva et al., 2016). For instance, the POxylation of GO can increase nanosheets' hydrophilicity and colloidal stability (De Melo-Diogo et al., 2018a). Moreira et al. demonstrated that the coating of AuMSS nanorods with POx improves nanomaterials' biocompatibility (Moreira et al., 2018b). Alternatively, the nanomaterials' coating with cells' membranes has also been explored (Fang et al., 2018). In this regard, RBCs' and macrophages' membranes have been investigated as alternatives to polymeric-based coatings (Gao et al., 2013; Zhang et al., 2018). Xuan et al. demonstrated that the coating of gold nanoshells with macrophages' membranes improves their blood circulation time and tumor accumulation from $\approx$ 1.6% to $\approx$ 7.5% ID/g (Xuan et al., 2016).

10.2.5 Targeting

Apart from the nanoparticles' innate capacity to accumulate within the tumor microenvironment by exploiting the defects of the tumor vasculature, their surface can also contain targeting moieties (e.g., small molecules and antibodies) to further improve their selectivity (Lima-Sousa et al., 2018; Stuchinskaya et al., 2011). In this regard, nanomaterials can be functionalized with ligands that bind to receptors overexpressed by the tumor vasculature's endothelial cells, leading to an improved accumulation at the target site (Li et al., 2015a; Deng et al., 2018). Shi et al. demonstrated that the functionalization of PEGylated reduced graphene oxide (rGO) with TRC105 (targets the CD105 overexpressed on the tumor's vasculature endothelial cells) increases the nanomaterial's tumor uptake from 2.7% to 5.6% ID/g (Shi et al., 2013a).

On the other hand, the targeting moieties can be directed to receptors overexpressed by cancer cells, therefore facilitating nanomaterials' interaction with these cells (Lima-Sousa et al., 2018; Chen et al., 2007). For this purpose, gold-, silica-, and graphene-based materials have been decorated with different molecules, such as folic acid, RGD peptides, AS1411, monoclonal antibodies, and hyaluronic acid (Qin et al., 2013; Kang et al., 2010; Tang et al., 2015; Eck et al., 2008; Lima-Sousa et al., 2018). In this context, Lima-Sousa et al. demonstrated that the functionalization of rGO with hyaluronic acid can improve the nanosheets' selectivity toward CD44 overexpressing cells (Lima-Sousa et al., 2018). In another work, AuMSS functionalization with AS1411 enhanced nanostructures' targeting to nucleolin overexpressing cancer cells (Zhang et al., 2015c). As demonstrated by Jang et al., nanomaterials' decoration with more than one targeting ligand (RGD and folate) can also result in an improved uptake by cancer cells when compared with single-ligand functionalized materials (Jang et al., 2015).

Nevertheless, nanomaterials decoration with targeting ligands is not a straightforward process. The nanomaterials' targeting capacity depends on the length of the spacer arm to which the ligand is connected and on the degree of grafting of the ligand

(Liu et al., 2011; Lee et al., 2015). For instance, Lee et al. verified that GO decorated with folate densities of 50% and 100% have a superior tumor uptake than GO functionalized with lower folate densities (10% or 25%) (Lee et al., 2015). Another concern related to the use of targeted nanomaterials lays on the fact that the protein corona can shield the ligand, rendering the targeting ineffective (Salvati et al., 2013). This limitation can be surpassed by functionalizing the nanomaterials with ligands that are protected during blood circulation and that only become available to interact with their receptor when exposed to a tumor microenvironment stimuli (Chien et al., 2013). For instance, Chien et al. produced PEGylated silica-coated upconversion nanoparticles functionalized with folic acid shielded with 2-nitrobenzylamine hydrochloride (cage molecule). When irradiated with near infrared (NIR) light, the cage molecule was released allowing an improved uptake mediated by the interaction of folic acid with the cancer cells (Chien et al., 2013).

10.3 Silica nanoparticles

10.3.1 General properties and synthesis of the different mesoporous silica-based nanoparticles

MSNs are one of the most explored inorganic structures for mediating the delivery of therapeutic agents. The MSNs contain a unique honeycomb-like mesoporous structure (Douroumis et al., 2013; Li et al., 2012). These mesopores are parallel tubular channels with a large volume ($>0.6\ cm^3/g$) and with an uniform and tunable pore size (2−10 nm) that can act as a reservoir to load anticancer agents (e.g., drugs) (Li et al., 2012). Furthermore, MSNs present an excellent thermal stability, good biocompatibility, and adjustable size (Li et al., 2012) (Table 10.1).

The synthesis of MSNs is based on a sol−gel method adapted from the original Stöber protocol (Stöber et al., 1968). In this method, a silica precursor [e.g., tetramethyl orthosilicate, tetraethyl orthosilicate (TEOS), or other] is added to a heated basic solution containing the pore structuring agent, usually the hexadecyltrimethylammonium bromide (CTAB) (Grün et al., 1997). In this reaction, the silica precursor undergoes a base-catalyzed hydrolysis reaction (removal of its alkoxy group) and starts to condensate on the surface of the cationic micelles formed by the CTAB (Grün et al., 1997). This condensation process is mediated by the electrostatic interactions established between the cationic surfactant template and the anionic silica species (Wu et al., 2013). The assemble of different silica-coated CTAB micelles results in the formation of the MSNs. Then, the MSNs are subjected to a solvent extraction method or calcination procedure to remove the CTAB, rendering nanoparticles with a highly ordered hexagonal porous structure available for the encapsulation of therapeutic agents (Rodrigues et al., 2019b; Reis et al., 2019; Moreira et al., 2018b). Additionally, the MSNs large surface area conjugated with the presence of silanol surface groups enables their easy modification with polymers and targeting agents for achieving an improved tumor uptake and selectivity toward cancer cells (Moreira et al., 2016). Furthermore, MSNs can also be conjugated with other organic or inorganic materials that will act as pore gatekeepers to produce stimuli-responsive anticancer agents (Niedermayer et al., 2015; Chen et al., 2014).

10.3.2 Mesoporous silica nanoparticle application in cancer therapy

The MSNs capacity to encapsulate high payloads of one or multiple therapeutic agents instigated their application as drug delivery systems for cancer chemo- and/or photodynamic therapy. The MSNs' drug loading is commonly achieved by promoting drug-nanoparticle hydrophobic interactions and/or the formation of hydrogen bonds. Further, the MSNs' stable and rigid framework allows the utilization of different methodologies as well as aqueous or organic solvents to achieve the maximum loading efficiency. Charnay et al. studied the effect of different solvents (e.g., DMSO, ethanol, and hexane) and methodologies (simple impregnation or impregnation/drying cycles) on the MSNs' loading with ibuprofen (Charnay et al., 2004). Their results showed that the use of less polar solvents facilitates the ibuprofen encapsulation on MSNs (ethanol: 184 mg/g; hexane: 590 mg/g; DMSO: 25.5 mg/g). Additionally, the ibuprofen encapsulation using ethanol as solvent was further improved with the successive impregnation/drying cycles, reaching the 1350 mg/g after four impregnations. In turn, Zhang et al. reported the MSNs-mediated delivery of the photosensitizer chlorin e6 and cisplatin prodrug for the chemophotodynamic therapy of cisplatin resistant A549 cancer cells (Zhang et al., 2016). In in vitro studies, the MSNs administration to the cancer cells resulted in an increased cisplatin uptake and mediated the production of high reactive oxygen species (ROS) levels upon exposition to 600 nm light, which translated in a severe reduction of A549 cells' viability.

Nevertheless, the application of drug-loaded MSNs in cancer therapy is severely hindered by the uncontrolled release profile of the therapeutic cargo. Therefore the MSNs have been combined with stimuli-sensitive (e.g., pH, redox, and temperature) materials that will act as pore gatekeepers preventing the drug premature release and subsequently, drug undesired interactions. For instance, Moreira et al. produced calcium carbonate-coated MSNs for the pH-sensitive delivery of doxorubicin (DOX) and ibuprofen to PC-3 cancer cells (Moreira et al., 2014). The calcium carbonate pH-dependent dissociation resulted in a faster drug release at pH 5.6 (30% of DOX released at 24 h), contrasting with the less than 10% recorded at pH 7.4. Such behavior favored the drugs accumulation in the interior of prostate cancer cells rendering an improved cytotoxic effect (Fig. 10.2). Li et al. observed that the grafting of a peptide containing an RGD sequence on the MSNs' surface through the formation of disulfide bonds could control the DOX release in function of the glutathione concentration (Li et al., 2015b). This control over the DOX release conjugated with the RGD targeting capacity resulted in an enhanced therapeutic effect toward U87 MG cancer cells.

The MSNs can also be tailored to be applied in cancer gene therapy. In this field, the loading of genetic material has been achieved by producing large pore-sized MSNs or by promoting the genetic material complexation with cationic materials attached at the nanoparticle surface. Meng et al. reported the codelivery of DOX and siRNA to breast cancer cells using MSNs functionalized with a PEG and polyethylenimine (PEI) copolymer (Meng et al., 2013). In this approach, the DOX was loaded in the MSNs pores whereas the Pgp siRNA was complexed with PEI at the nanoparticles' surface. In vivo, the MSNs combined gene and drug delivery resulted in a tumor inhibition rate of 80%, whereas the free DOX and DOX-loaded MSNs presented a tumor inhibition rate of 17% and 62%, respectively.

The in vitro and in vivo imaging of cancer cells can also be mediated by MSNs by exploring the nanoparticles doping or surface modification with imaging agents

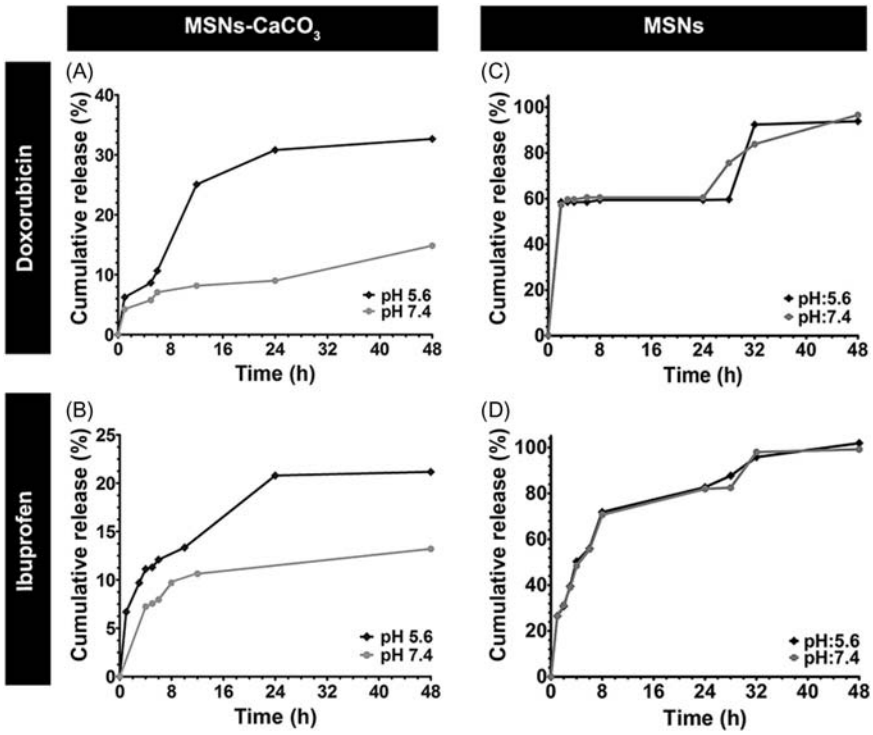

FIGURE 10.2 Drug release profile of pH-sensitive MSNs coated with calcium carbonate ($CaCO_3$). The MSNs with or without $CaCO_3$ were incubated at pH 7.4 to mimic the physiological conditions and at pH 5.6 to simulate the acidic tumor microenvironment. The release of doxorubicin (A) and ibuprofen (B) from the pH-responsive MSNs-$CaCO_3$ was faster at pH 5.6. In contrast, no significative differences were observed in the release of doxorubicin (C) and ibuprofen (D) from the MSNs at both pHs. Source*: Reprinted from Moreira, A.F., Gaspar, V.M., Costa, E.C., De Melo-Diogo, D., Machado, P., Paquete, C.M., Correia, I.J., 2014. Preparation of end-capped pH-sensitive mesoporous silica nanocarriers for on-demand drug delivery. Eur. J. Pharm. Biopharm. 88(3), 1018, with permission from Elsevier.*

(fluorescein isothiocyanate, IR-820, and gadolinium) (Qian et al., 2012; Zhang et al., 2015a; Huang et al., 2010). Zhang et al. observed that the DOX-loaded MSNs functionalized with PEI chains containing gadolinium and folic acid could efficiently increase the magnetic resonance contrast in tumor cells (HeLa cells) (Zhang et al., 2015a). Furthermore, the MSNs imaging [application in Raman, computed tomography (CT), and magnetic resonance] and therapeutic (photothermal therapy) potential can be further improved by conjugating them with other nanomaterials such as gold, iron oxide, and graphene (reviewed in Sections 10.6.1 and 10.6.2).

10.4 Gold nanoparticles

10.4.1 General properties and synthesis

Gold nanomaterials have been explored in multiple applications such as drug delivery, photothermal therapy, and imaging (Huang et al., 2011; Jain et al., 2012). The gold is a

material resistant to corrosion, oxidation, and degradation, and one of the least reactive known metals (Yang et al., 2015). Further, the gold nanoparticles' surface plasmon resonance (SPR) phenomenon (i.e., the synchronized oscillation of the particles' free electrons upon their exposition to a beam of light corresponding to their resonance wavelength, which leads to light scattering or absorption) enables their use in multiple medical applications as imaging and/or absorptive heating agents (Huang and El-Sayed, 2010; Yang et al., 2015; Huang et al., 2007). This phenomenon can be modulated in gold nanomaterials by fine-tuning the synthesis procedure and consequently, their size and shape (Huang and El-Sayed, 2010; Li et al., 2014a). Additionally, the gold nanoparticles affinity to interact with compounds presenting thiol (−SH) and disulfide (S−S) groups allow their straightforward functionalization with polymers or targeting moieties (Love et al., 2005; Liu and Peng, 2017; Yang et al., 2015) (Table 10.1).

The production of gold nanomaterials can be achieved through different synthetic routes rendering nanoparticles with different sizes and shapes (Li et al., 2014a; Yang et al., 2015). Nevertheless, most of the methods are based on the reduction of the gold salt followed by the gold atoms nucleation in the presence of a stabilizing agent to prevent the formation of aggregates (Zhao et al., 2013; Moreira et al., 2018a). The spherical-shaped particles are obtained when the synthesis is conducted in thermodynamically controlled conditions (Kundu et al., 2009; Moreira et al., 2018a). To produce nonspherical gold nanoparticles, the gold atoms nucleation must occur in an anisotropic manner. Such is usually achieved by using agents that block some of the gold nucleation growing directions (Li et al., 2014a; Yang et al., 2015). For instance, gold nanorods are produced by adding small gold nanospheres to a solution containing a gold salt (e.g., chloroauric acid), CTAB, a weak reducing agent, and silver nitrate to induce the rod-shaped growth (Lohse and Murphy, 2013; Rodrigues et al., 2019a). On the other hand, gold nanostars can be produced by promoting the gold nucleation on poly(vinyl pyrrolidone)-coated small gold nanospheres in the presence of dimethylformamide, whereas gold nanocages are prepared using a galvanic replacement process based on sacrificial silver nanocubes (Chandra et al., 2016; Xia and Xia, 2014; Zhao et al., 2013).

10.4.2 Gold nanoparticles in cancer therapy

Gold nanomaterials have been widely explored for imaging applications (Li and Chen, 2015; Cole et al., 2015; Cheng et al., 2017). The high density and X-ray absorption coefficient of gold allows their use as contrast agents in CT (Cole et al., 2015; Wen et al., 2013). In fact, gold nanoparticles can outperform conventional contrast agents. For example, when compared with iodine (one of the most used contrast agents), the gold absorption coefficient upon irradiation with an X-ray beam of 100 keV is more than two times superior (Xi et al., 2012). Contrary to the conventional contrast agents, gold nanoparticles can take advantage from the EPR effect, enabling tumor imaging for long periods of time (nanomaterials are slowly removed from the tumor site when compared with small molecules) (Cole et al., 2015; Cheng et al., 2017). Gold nanomaterials can also be functionalized with targeting ligands, which further increases their selectivity to the tumor tissue and enables the detection of cancer metastasis (Reuveni et al., 2011; Peiris et al., 2015). For example, Wang et al. developed folic acid−modified dendrimer-entrapped gold nanoparticles for in vitro and in vivo targeted CT imaging of lung adenocarcinomas (Wang et al., 2013a).

The excellent optical properties that characterize the gold nanoparticles are related to their SPR. In fact, the optimization of gold nanoparticles size and shape (e.g., spheres, cages, stars, rods triangles, or others) allows the gold nanoparticles' SPR wavelength tuning to the NIR region (700−1100 nm). In this way, the absorption of NIR light by gold nanomaterials enables their application as photothermal agents (NIR light has minimal/insignificant interactions with biological components) (Akhter et al., 2012; Alex and Tiwari, 2015). In this type of therapy, if a temperature increase to 41°C−45°C is attained, cancer cells can suffer mild alterations on their metabolic functions, experience impairment in the DNA repair mechanisms, or become sensitized to the action of other agents (Chu and Dupuy, 2014). In contrast, when the temperature reaches 50°C (or above), the cells' functions are severely affected, ultimately leading to their death by necrosis (Chu and Dupuy, 2014).

Generally, gold nanospheres are not suited for cancer photothermal therapy since their absorption peak occurs between 500 and 550 nm (Alex and Tiwari, 2015). On the other hand, rod-shaped gold nanoparticles present two distinct bands in their absorption spectrum that are related to their two orientations. Gold nanorods' axial absorption band is similar to that of spherical particles (500−550 nm), while the longitudinal absorption band has a strong absorption in the NIR region (Alex and Tiwari, 2015; Huang and El-Sayed, 2010). The increase in rod particles' aspect ratio (length/width) can produce a shift to even higher wavelengths (Huang and El-Sayed, 2010; Tong et al., 2017; Mackey et al., 2014). For instance, Wang et al. explored the use of DNA-wrapped gold nanorods in cancer therapy, verifying that the combination of these materials with NIR light (photothermal effect) could induce a reduction in the tumor's growth and diminish the occurrence of lung metastasis (Wang et al., 2014). Besides gold nanorods, gold nanostars, gold nanocages, and nanoclusters are also being applied for cancer photothermal therapy due to their NIR absorption (Xia and Xia, 2014; Liu et al., 2015c; Sun et al., 2017b; Chandra et al., 2016). Even though gold nanoparticles can suffer photodegradation upon NIR laser irradiation (Chen et al., 2010), such phenomenon can be suppressed by modifying particles' surface with other inorganic materials such as silica (Moreira et al., 2018a) (reviewed in Section 10.6.1).

Still, the use of gold nanoparticles for cancer theragnostic requires their functionalization. In fact, as-synthesized gold structures have a high toxicity due to the presence of CTAB (Dreaden et al., 2012; Yasun et al., 2015). This limitation can be surpassed by functionalizing the nanoparticles with biocompatible polymers (for instance using thiol-exchange chemistry) (Woehrle et al., 2005; Gao et al., 2012). Furthermore, as-synthesized gold structures also display a low stability in biological fluids and tend to aggregate (Dreaden et al., 2012; Chegel et al., 2012). Gold nanoparticles' functionalization can also overcome these drawbacks (Guerrini et al., 2018). In this regard, PEGylation is one of the most common strategies to prevent gold nanoparticles aggregation, avoid protein adsorption, and improve the tumor uptake (Ding et al., 2013; Yang et al., 2014).

Moreover, gold nanoparticles' surface modification with polycations (e.g., PEI) enable their use in gene delivery, polymer−drug conjugates or directly conjugated with small molecules for drug delivery applications (Farooq et al., 2018; Aryal et al., 2009). It is also possible to incorporate therapeutic agents on functionalized-gold nanoparticles through

electrostatic interactions (Mirza and Shamshad, 2011). For instance, Wang et al. described the DOX delivery to breast cancer cells using gold nanospheres (Wang et al., 2011b). In this approach, DOX was immobilized in the gold surface using PEG as a spacer arm. In vitro assays demonstrated that this approach could enhance the drug accumulation and retention in multidrug resistant MCF-7/ADR cancer cells as well as increase their therapeutic efficacy.

10.5 Graphene family nanomaterials (GFN)

10.5.1 General properties and synthesis of the different GFN

GO and rGO are the most commonly applied graphene family nanomaterials in cancer therapy. GO is a 2D material with a graphitic structure decorated with oxygen-containing groups (e.g., epoxy, hydroxyl, and carboxyl groups) (Chen et al., 2012; De Melo-Diogo et al., 2017a; Shim et al., 2016). The aromatic lattice and high surface area of GO and rGO make them an excellent platform to encapsulate different compounds for cancer therapy purposes (e.g., drugs, photodynamic, and immunotherapy agents) through hydrophobic–hydrophobic interactions and/or $\pi-\pi$ stacking (Wu et al., 2015; De Melo-Diogo et al., 2018a; Yi et al., 2019; Patel et al., 2016). As importantly, GO and rGO display NIR absorption, enabling their use in cancer photothermal therapy (Yang et al., 2013; Yi et al., 2019; De Melo-Diogo et al., 2017a; Lima-Sousa et al., 2018) (Table 10.1).

GO is generally produced through the chemical oxidation of graphite followed by the exfoliation of the resulting material until nanosheets are attained (Marcano et al., 2010). The improved Hummer's method, which uses sulfuric acid, phosphoric acid, and potassium permanganate in the oxidation of graphite, is the most commonly employed method to produce GO (Marcano et al., 2010). rGO is usually obtained by treating GO with reducing agents, a process that restores the materials' graphitic lattice (by removing the oxygen-functional groups) and thereby improving their photothermal and loading capacity (Pei and Cheng, 2012). In this regard, hydrazine hydrate is generally used to perform the reduction of GO (Robinson et al., 2011; Pei and Cheng, 2012). Recently, Lima-Sousa et al. demonstrated that L-ascorbic acid can also be used to produce rGO with improved stability and size distribution for cancer therapy (Lima-Sousa et al., 2018).

Despite the potential of GO and rGO, these materials present several limitations. Even though GO has some aqueous solubility due to its oxygen-functional groups, this material precipitates in biological fluids (Sahu et al., 2013; Liu et al., 2008; Li et al., 2014b). Furthermore, rGO has a limited solubility (depends on the method used for its reduction) and also aggregates in biological media (Li et al., 2014b). Both GO and rGO have a low biocompatibility/hemocompatibility, suboptimal tumor accumulation, and lack selectivity toward cancer cells (De Melo-Diogo et al., 2018b).

These limitations can be surpassed by functionalizing GO surface with biocompatible polymers capable of improving nanostructures' blood circulation time and selectivity toward cancer cells (De Melo-Diogo et al., 2018b). To accomplish that, GO nanomaterials functionalization has been performed through the covalent bonding of materials terminated with primary amine groups ($-NH_2$) to the carboxyl groups of GO using the carbodiimide chemistry

(Yang et al., 2010; Tian et al., 2016). Alternatively, the problems associated with rGO can be addressed by coating it with amphiphilic polymers through the establishment of hydrophobic−hydrophobic interactions and/or π−π stacking (Lima-Sousa et al., 2018; Liu et al., 2017).

10.5.2 Graphene family nanomaterials application in cancer therapy

The NIR absorption of GO and rGO has propelled their use in cancer photothermal therapy. In this type of application, rGO can produce a higher temperature increase upon irradiation than GO, due to its higher NIR absorption (Lima-Sousa et al., 2018). Yang et al. compared the performance of PEGylated rGO and PEGylated GO, verifying that the former could induce the total tumor ablation upon NIR laser irradiation due to its higher tumor-homing capacity and greater photothermal capacity (Yang et al., 2012b). Lima-Sousa et al. functionalized rGO with a hyaluronic acid−based amphiphilic polymer, verifying that this material could produce a photoinduced heat of 33°C (Lima-Sousa et al., 2018). In in vitro studies, the hyaluronic acid−functionalized rGO displayed a preferential uptake by CD44 overexpressing cancer cells, mediating a reduction on their viability to 6% upon NIR laser irradiation (Lima-Sousa et al., 2018).

The aromatic lattice of GO/rGO allows the incorporation of photosensitizers (usually hydrophobic small molecules that produce ROS upon irradiation) through noncovalent interactions (Sahu et al., 2013). Alternatively, the photosensitizers may be covalently conjugated to polymer-functionalized GO (Luo et al., 2016b). In this way, several photosensitizers have been loaded on GO/rGO for application in cancer photodynamic-photothermal therapy (Luo et al., 2016b; Tian et al., 2011; Dos Santos et al., 2018; Zhang et al., 2017). Luo et al. covalently conjugated the photosensitizer IR-808 to GO dual-functionalized with PEG and PEI (IR-808-PEI-PEG-GO), verifying that the photodynamic-photothermal effect mediated by this material upon NIR laser irradiation led to the complete tumor eradication (Luo et al., 2016b). In contrast, tumor growth reduction was observed for mice treated with only photothermal (PEI-PEG-GO + NIR) or photodynamic (IR-808 + NIR light) therapies. Tian et al. also observed that the combined photodynamic-photothermal effect mediated by Pluronic F127-functionalized GO loaded with the photosensitizer Methylene Blue produces an enhanced therapeutic effect when compared with single phototherapies (Tian et al., 2011).

The aromatic lattice of GO/rGO also enables the loading of chemotherapeutics through hydrophobic−hydrophobic interactions and π−π stacking (De Melo-Diogo et al., 2018a; Liu et al., 2013, 2017; Shim et al., 2016; Hu et al., 2018; Tran et al., 2015). For instance, De Melo-Diogo et al. loaded a dual drug combination in POxylated GO (De Melo-Diogo et al., 2018a). The in vitro studies revealed that the chemophotothermal effect mediated by the dual drug-loaded POxylated GO induced a superior therapeutic outcome when compared with the action of photothermal (POxylated GO + NIR) and chemotherapy-based treatments (free-drug combination and dual drug delivery by POxylated GO) (De Melo-Diogo et al., 2018a) (Fig. 10.3).

The functionalization of GO and rGO with polycations enables their electrostatic complexation with the negatively charged genetic material. For this purpose, chitosan-, PEI-, and poly(allylamine hydrochloride) (PAH)-based materials can be used to functionalize

TABLE 10.1 Overview of MSNs, gold, and GFN general properties, main applications, and limitations.

Nanoparticles	General properties	Main application	Limitations	References
MSNs	Unique honeycomb-like mesoporous structure, Large surface area, Channels with a large volume and uniform pore size, Excellent thermal stability, Good biocompatibility, Tunable size and surfaces, High loading capacity.	Chemotherapeutics and photodynamic agents' delivery.	Premature drug release, Suboptimal tumor accumulation, Lack of selectivity toward cancer cells.	Moreira et al. (2016), Bharti et al. (2015)
Gold nanomaterials	Biocompatible and nonreactive material, Tunable SPR, Easy surface functionalization, Tunable size and shape, Shape-dependent optical properties.	Contrast agents in bioimaging (CT, X-ray, magnetic resonance imaging), Photothermal therapy.	Interaction with thiol or disulfide groups, which leads to biomolecules' adsorption on the nanoparticle surface, Low loading capacity, Premature drug release, Photothermal degradation, Suboptimal tumor accumulation, Lack of selectivity toward cancer cells, Low scalability of the anisotropic shapes synthesis.	Akhter et al. (2012), Moreira et al. (2018a), Huang and El-Sayed (2010), Yang et al. (2015)
GFN	High surface area, NIR absorption, Some solubility due to its oxygen-functional groups (GO), Easy surface functionalization, Raman imaging capacity.	Photothermal therapy, Chemotherapeutics and photodynamic agents' delivery.	Limited solubility and aggregation in biological fluids, Premature drug release, Low biocompatibility, Suboptimal tumor accumulation, Lack of selectivity toward cancer cells.	Zhu et al. (2010), De Melo-Diogo et al. (2018b)

GO/rGO (Bao et al., 2011; Feng et al., 2013; Wu et al., 2017; Chen et al., 2011; Yin et al., 2017). For instance, Yin et al. developed folate-PEG-GO complexed with PAH and with HDAC1 and K-Ras siRNAs (Yin et al., 2017). In vivo, the combined gene delivery and photothermal effect mediated by this nanoformulation produced a superior cytotoxic effect when compared with the stand-alone therapies (gene therapy: HDAC1 and K-Ras siRNA complexed PAH/folate-PEG-GO; photothermal therapy: PAH/FA-PEG-GO + NIR light) (Yin et al., 2017).

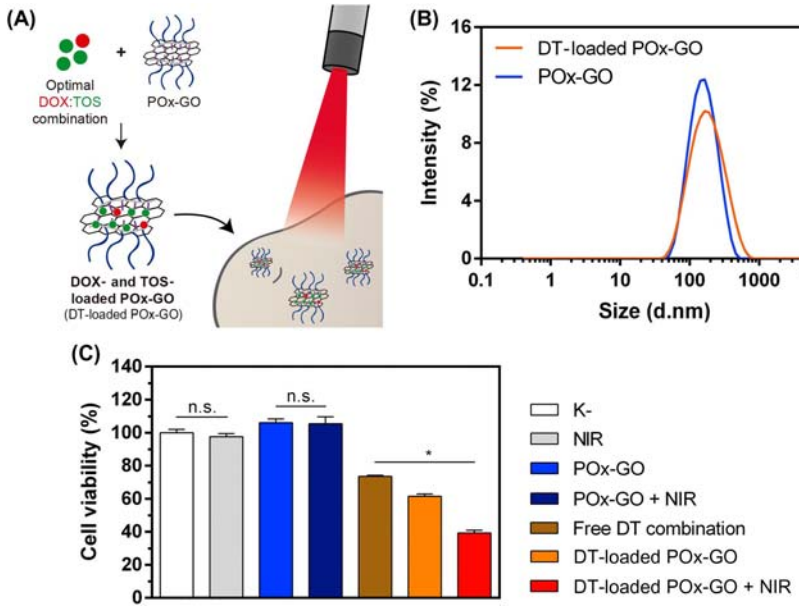

FIGURE 10.3 Application of DOX and α-tocopheryl succinate loaded POxylated GO (DT loaded POx-GO) in cancer chemophotothermal therapy. Schematic representation of the cancer therapy mediated by DT loaded POx-GO (A). Dynamic light scattering analysis of the POx-GO and DT loaded POx-GO sizes distribution. It can be observed that the encapsulation of the drug combination in the POx-GO did not induce significant changes on the nanomaterials' size distribution (B). Analysis of the stand-alone and the therapeutic effects mediated by POx-GO and DT loaded POx-GO in the presence (+NIR) and absence of NIR light toward breast cancer cells. The chemophototherapeutic effect mediated by DT loaded POx-GO induced a stronger reduction on cells viability, when compared with the stand-alone therapies (C). K^- and NIR denote the negative control and the NIR light treated cells, respectively. Source: *Reprinted from De Melo-Diogo, D., Costa, E.C., Alves, C.G., Lima-Sousa, R., Ferreira, P., Louro, R.O., Correia, I.J., 2018. POxylated graphene oxide nanomaterials for combination chemo-phototherapy of breast cancer cells. Euro. J. Pharm. Biopharm. 131, 167, with permission from Elsevier.*

Furthermore, GO/rGO have recently started to be loaded with immune checkpoint inhibitors [e.g., indoleamine 2,3-dioxygenase inhibitor using hydrophobic−hydrophobic interactions and π−π stacking (Yan et al., 2018)] or immunostimulatory agents [e.g., cytosine−phosphate−guanine oligodeoxynucleotides by electrostatic interactions with polycation-functionalized GO (Tao et al., 2014)] for application in cancer immunophotothermal therapy.

Finally, GO and rGO can also be explored for imaging applications. For this purpose, the Raman signature of these materials enables their use in Raman imaging (Lin et al., 2018). Furthermore, gold nanoparticles can also be grown on GO/rGO surface (reviewed in Section 10.6.3), improving materials' Raman imaging capacity and also endowing them with capacity for CT imaging (Sun et al., 2017a). Similarly, iron oxide nanoparticle can also be grown on these materials for magnetic resonance imaging (Yang et al., 2012a). On the other hand, GO/rGO can also be labeled with fluorescent probes (for fluorescence imaging) and radionuclides (for positron emission tomography) (Lin et al., 2018).

10.6 Hybrid nanoparticles

10.6.1 Gold core silica shell nanoparticles

The coating of gold nanoparticles with an MSS can address gold nanoparticles' limitations and is a promising route to prepare multifunctional anticancer nanosystems (Ghosh Chaudhuri and Paria, 2011). The inclusion of the MSS on gold nanoparticles (AuMSS) yields hybrids with an enhanced colloidal stability in contact with the body fluids and with improved photostability (Kanehara et al., 2009; Chen et al., 2013).

Furthermore, the MSS provides a chemically inert and biocompatible surface (by replacing the CTAB) and protects the gold core from photothermal degradation (Mamaeva et al., 2013; Moreira et al., 2018a). Apart from the gold core capacity to perform imaging and photothermal therapy, the pores that constitute the MSS can act as reservoirs for pharmaceutical agents. Such allows the encapsulation of different bioactive molecules (e.g., drugs, DNA, proteins, fluorescent probes, others) on AuMSS pores and promotes their application as multifunctional systems (Song et al., 2015; Moreira et al., 2018b; Wang et al., 2015c). Additionally, the MSS has a high surface area that can be easily functionalized with different stimuli-responsive materials or targeting agents (Rodrigues et al., 2019a; Moreira et al., 2014; Luo et al., 2016a; Zhou et al., 2017). Such allows the assembly of AuMSS hybrids with a high tumor uptake, selectivity toward cancer cells, and responsiveness to specific stimulus of the tumor microenvironment (e.g., pH, temperature, ROS, enzymes) (Rodrigues et al., 2019a, 2019b) (Table 10.2).

The AuMSS nanoparticles' synthesis can be divided into two phases: the production of the gold core with the desired shape and size (as described in Section 10.4.1) and the coating with a silica shell (Dias et al., 2016; Moreira et al., 2018a). Briefly, after the gold core synthesis, the coating with MSS is performed through the Stöber method or its derivations (Kobayashi et al., 2001). During this procedure, the silica precursor (e.g., TEOS) condensates around the gold core by electrostatic interactions (CTAB on the gold nanoparticles' surface is positively charged and the silica molecules are negatively charged) originating the MSS. Further, during the condensation reaction, the additional CTAB micelles present on the media will act as pore structuring agents (Kobayashi et al., 2001; Mine et al., 2003).

AuMSS can assume rod, star, and cage shapes (anisotropic shapes), displaying absorbance peaks in the NIR region and therefore allowing their application in cancer photothermal therapy (Moreira et al., 2018a). The silica shell is optically transparent to the NIR radiation, a fact that indicates that gold core' modification with the MSS does not compromise the nanostructures' photothermal capacity (Song et al., 2015; Ghosh Chaudhuri and Paria, 2011). In fact, some studies have reported that the incorporation of the MSS leads to a slight shift on the absorption peaks to the NIR region, which may contribute to a better thermal ablation of the tumors (Liu et al., 2015b). Additionally, anisotropic AuMSS can also be loaded with chemotherapeutic drugs for application in cancer chemophotothermal therapy (Moreira et al., 2018b; Hu et al., 2015; An et al., 2017). For this purpose, drugs are loaded on AuMSS by covalent bonding or electrostatic interactions with the silica shell's pores (Zhou et al., 2018; Kesse et al., 2019). Therefore it is also crucial to coat AuMSS pores to achieve a controlled drug release and avoid drug leakage during blood circulation (Rodrigues et al., 2019a).

TABLE 10.2 Overview of AuMSS; GFN−MSS, and GFN-gold nanohybrids' general properties; main applications; and limitations.

Nanoparticles	General properties	Main application	Limitations	References
AuMSS	Increased colloidal stability, Increased the biocompatibility, Large surface area and pores which can be easily modified, Protection of the gold core from photothermal degradation.	Photothermal therapy, Chemotherapeutics agents' delivery, Bioimaging.	Premature drug leakage, Low scalability of the anisotropic shapes synthesis, Suboptimal tumor accumulation, Lack of selectivity toward cancer cells.	Moreira et al. (2018a), Rodrigues et al. (2019a)
GFN−MSS	Improved colloidal stability, Improved biocompatibility, Improved loading capacity.	Photothermal therapy, Chemotherapeutics agents' delivery.	Premature drug release, Suboptimal tumor accumulation, Lack of tumor selectivity.	Wang et al. (2013c)
GFN-gold nanohybrids	Increased photothermal capacity, Increased Raman imaging capacity.	Photothermal therapy, Chemotherapeutics and photodynamic agents' delivery, Bioimaging.	Low loading capacity, Premature drug release, Limited solubility and aggregation in biological fluids, Photodegradation, Suboptimal tumor accumulation, Lack of tumor selectivity.	Khalil et al. (2016)

Recently, Moreira et al. prepared DOX-loaded POx-functionalized rod-shaped AuMSS for application in cancer chemophotothermal therapy (Moreira et al., 2018b). The POx coating improved nanostructures' hemocompatibility. Furthermore, the drug delivery mediated by AuMSS-POx led to a 220% increase in DOX uptake by cancer cells when compared with the free DOX. In the in vitro studies, the chemophotothermal cytotoxic effect mediated by AuMSS-POx was superior to that attained by the single-therapies (photothermal therapy: AuMSS-POx + NIR; chemotherapy: DOX-loaded AuMSS-POx) (Moreira et al., 2018b). In another work, Reis et al. also verified that the coating of AuMSS nanospheres with POx and β-cyclodextrins improves nanospheres' cytocompatibility, hemocompatibility and uptake by cancer cells, being a promising hybrid agent for theragnostics (Reis et al., 2019) (Fig. 10.4). Moreover, Zhang et al. developed pH-responsive AuMSS nanorods to deliver DOX to cervical cancer cells, in a more specific and controlled manner (Zhang et al., 2015b). For this purpose, the DOX was chemically linked to the mesoporous shell through a Schiff base bonding (acid-labile bound). The authors reported that this bonding prevented the DOX release from silica pores at pH 7.4. However, approximately 70% of DOX was released when nanoparticles were incubated at pH 5, thus showing that they may mediate a tumor confined drug release. Luo et al. prepared AlPcS4-loaded (660 nm light responsive photosensitizer) rod-shaped AuMSS dual-functionalized with

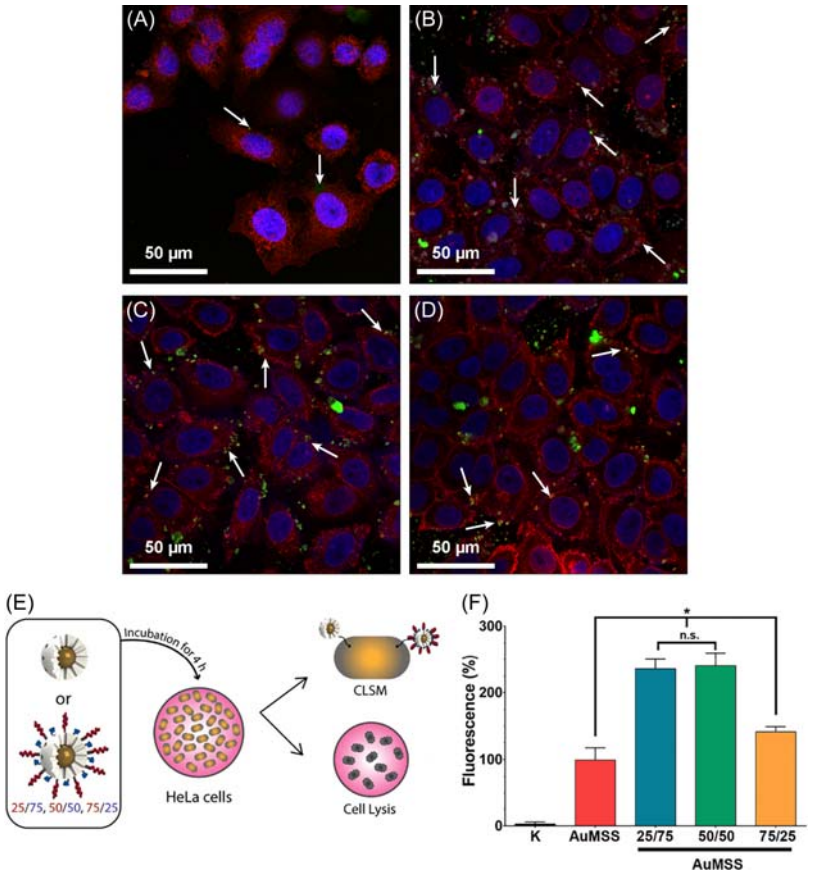

FIGURE 10.4 Cellular uptake analysis of the AuMSS nanospheres functionalized with different POx/β-cyclodextrins weight ratios. Representative confocal microscopy images of the FTIC labeled AuMSS (A), AuMSS 25/75 (B), AuMSS 50/50 (C), and AuMSS 75/25 (D) formulations uptake after 4 h of incubation with HeLa cells. Red channel: WGA-Alexa Fluor 594 stained cell cytoplasm; Blue channel: nucleus stained with Hoechst 33342; Green channel: FITC labeled nanoparticles. The white arrows are pointing to the internalized nanoparticles. These confocal images show the presence of the nanoparticles in the cells' cytoplasm, indicating that the AuMSS functionalization may improve their internalization. To corroborate these results, fluorescence spectroscopy analysis was performed simultaneously with the confocal microscopy analysis (E). The AuMSS nanospheres formulations' fluorescence analysis showed that the AuMSS 25/75 and 50/50 formulations possess the highest cellular uptake (≈ 240%). Cells without nanoparticles incubation (K) were used as control (F). These results are in accordance with confocal data and confirm that POx and β-cyclodextrins coating improved the AuMSS uptake. Source: *Adapted from Reis, C.A., Rodrigues, C.F., Moreira, A.F., Jacinto, T.A., Ferreira, P., Correia, I.J., 2019. Development of gold-core silica shell nanospheres coated with poly-2-ethyl-oxazoline and β-cyclodextrin aimed for cancer therapy. Mater. Sci. Eng. C 98, 966–967, with permission from Elsevier.*

PEG-adamantine and lactobionic acid-adamantine through host–guest interactions with β-cyclodextrin-Pt(IV) conjugates immobilized on the particle surface (Luo et al., 2016a). This hybrid system presented a four times greater uptake by HepG2 cells (lactobionic acid receptor overexpressing liver cancer cells) when compared with COS7 cells

(kidney fibroblasts that do not overexpress lactobionic acid receptor). In vivo, the AuMSS presented a preferential accumulation in the tumor tissue and the chemophotodynamic-photothermal effect stalled the tumor growth (Luo et al., 2016a).

Furthermore, AuMSS intrinsic properties allow their application in CT, surface-enhanced Raman spectroscopy imaging, and photoacoustic imaging (for anisotropic AuMSS) (Xu et al., 2018; Seo et al., 2014). For instance, Kobayashi et al. produced AuMSS nanospheres with an attenuation coefficient capacity approximately seven times higher than that of the commercial iodine (Kobayashi et al., 2013). Additionally, the AuMSS conjugation with contrast agents (e.g., gadolinium, zirconium-89) also allows its application in magnetic resonance imaging and positron emission tomography. In this regard, Xu et al. prepared a multimodal theragnostic system by labeling DOX-loaded PEGylated AuMSS with the radioisotope zirconium-89 (Xu et al., 2018). In vivo, this system was able to perform dual-modality tumor imaging (photoacoustic imaging and positron emission tomography). Furthermore, the chemophotothermal effect mediated by this system induced tumor's regression, proving its theragnostic capacity.

10.6.2 Graphene family nanomaterials and mesoporous silica shell nanohybrids

The functionalization of rGO with MSS is a convenient route to surpass some limitations of the former. This type of functionalization can improve the rGO nanostructures' hydrophilicity and stability (Wang et al., 2013c). Furthermore, the MSS allows the loading of a wide variety of therapeutics in its pores, improving the loading capacity of GO and rGO (Wang et al., 2013c). In fact, the DOX loading capacity of rGO−MSS-based materials was 3.6 and 2.5−6.5 times higher than that of GO and rGO derivatives, respectively (Shao et al., 2017). The MSS also offers additional grafting sites for nanomaterials' functionalization (Wang et al., 2013c) (Table 10.2).

rGO−MSS can be synthesized using the CTAB-guided assembly of silica precursors (e.g., TEOS), hydrolyzed under basic conditions, on the GO surface (Wang et al., 2013c). The basic conditions employed in this procedure lead to the reduction of GO, yielding rGO−MSS hybrids (Wang et al., 2013c). Alternatively, dopamine has also been added to ensure the GO reduction (Liu et al., 2019). During rGO−MSS synthesis, silica precursors with primary amine groups (e.g., APTES) can also be used to yield hybrids with functional groups for polymer functionalization using the carbodiimide chemistry (e.g., NHS-PEG) or electrostatic complexation with negatively charged polymers (e.g., hyaluronic acid) (Wang et al., 2013c; Shao et al., 2017).

rGO−MSS have been explored for cancer chemophotothermal therapy by taking advantage from photothermal and loading capacities of rGO and MSS, respectively (Shao et al., 2017; Liu et al., 2019). In this context, Shao et al. investigated the therapeutic capacity of DOX-loaded hyaluronic acid−functionalized rGO−MSS (Shao et al., 2017). These hybrid nanostructures displayed an NIR- and pH-responsive DOX release mediated by the photothermal effect and the detachment of the hyaluronic acid coating (reduction of the electrostatic interactions between the amine groups of the rGO−MSS and hyaluronic acid), respectively. In vivo, these hybrids demonstrated a high tumor-homing capacity, mediating a synergistic chemophotothermal antitumoral effect.

Liu et al. also verified that rGO−MSS−poly(dopamine) hybrids loaded with DOX can be used for the NIR- and pH-responsive drug release (Liu et al., 2019). In another work, Wang et al. produced DOX-loaded IL-13-functionalized PEGylated rGO−MSS for the targeted cancer chemophotothermal therapy (Wang et al., 2013c). In in vitro studies, the hybrid structures demonstrated a higher uptake by glioblastoma cells when compared with normal cells, thus being able to induce a stronger reduction of cancer cells' viability.

10.6.3 Graphene family nanomaterials and gold nanohybrids

The preparation of GO/rGO-Au hybrids has been pursued by researchers to attain multifunctional imaging agents with improved photothermal capacity. GO/rGO-Au hybrids can be used for fluorescence imaging and CT (Wang et al., 2011a; Sun et al., 2017a; Shi et al., 2013b). Furthermore, these hybrids display enhanced Raman signals further augmenting their potential for Raman imaging (Sun and Wu, 2011; Kim et al., 2015). The incorporation of anisotropic gold nanoparticles (e.g., gold nanorods, gold nanostars) on GO/rGO leads to the assembly of hybrids with an improved NIR absorption and photothermal capacity (Sun et al., 2017a; Dembereldorj et al., 2014; Nergiz et al., 2014; Wang et al., 2016). Furthermore, the gold nanoparticles incorporated on graphene derivatives enable the hybrids straightforward covalent functionalization with thiolated polymers (e.g., mPEG-SH) (Shi et al., 2013b; Wang et al., 2016). Alternatively, GO/rGO-Au hybrids can also be functionalized through electrostatic or noncovalent interactions (Sun et al., 2017a; Kim et al., 2015) (Table 10.2).

The preparation of GO/rGO hybrids can be accomplished by adsorbing gold nanoparticles to the surface of graphene derivatives (Kang et al., 2017) or by promoting the in situ growth of these gold nanomaterials on the graphene derivatives' structure (Nergiz et al., 2014).

The GO/rGO-Au hybrids have been mostly explored for cancer photothermal therapy due to their enhanced photothermal capacity. Dembereldorj et al. demonstrated the applicability of PEGylated GO incorporating gold nanorods in cancer photothermal therapy (Dembereldorj et al., 2014). In a similar way, Kang et al. demonstrated that GO incorporating α-synuclein-coated AuNPs display a 2.5- and 1.6-fold higher photothermal capacity than GO and AuNPs, respectively (Kang et al., 2017).

The aromatic matrix of GO/rGO-Au hybrids also enables the loading of other agents for application in cancer multimodal therapy. In this regard, Wang et al. investigated the therapeutic capacity of DOX-loaded PEGylated rGO-Au nanostar hybrids (Wang et al., 2016). In vivo, the chemophotothermal effect mediated by these hybrids leads to the complete tumor eradication. In contrast, the sole application of chemotherapy (DOX-loaded PEGylated rGO-Au nanostars) or photothermal therapy (PEGylated rGO-Au nanostars + 655 nm laser light) only induced a reduction of the tumors' growth. In another work, Kim et al. verified that zinc phthalocyanine (660 nm light responsive photosensitizer)-loaded PEGylated GO-Au nanoparticle hybrids mediate a combined photodynamic-photothermal effect, upon interaction with 808 plus 660 nm light that induces the highest cytotoxicity on cancer cells (Kim et al., 2015).

10.7 Challenges and opportunities

In this chapter, the gold, MSNs, and GO/rGO-based nanoparticles' as well as their hybrids' application in cancer therapy and imaging were reviewed.

Overall, nanomaterials' size, charge, shape, and corona composition, as well as the presence of targeting ligands on their surface influence their ability to reach the tumor site, and hence their biological performance. Even though each parameter must be analyzed in a case-to-case basis, the passivation of nanomaterials' surface with stealth polymers and targeting agents appears to be the most efficient approach to improve nanostructures' tumor accumulation and selectivity.

These inorganic nanomaterials have been applied in different therapeutic modalities due to their intrinsic properties. The pores of MSNs have pushed their application in cancer drug delivery. Anisotropic gold nanoparticles have been explored in cancer photothermal therapy due to their NIR absorption. By coating anisotropic gold nanoparticles with an MSS, researchers have attained materials that can perform drug delivery and photothermal therapy as well as multimodal tumor imaging. On the other hand, the aromatic lattice of GO/rGO as well as their NIR absorption has enabled mainly their application in cancer chemophotothermal therapy. The coating of rGO with MSS greatly enhanced its drug delivery capacity. In turn, the adsorption of gold nanoparticles on GO/rGO led to the assembly of hybrids that can perform multimodal tumor imaging and enhanced photothermal therapy.

Despite the theragnostic potential of these inorganic nanoparticles, their clinical translation has been slow. The complexity of some of these materials poses a challenge to their large-scale production. On the other hand, the nonbiodegradability of these materials also raises concerns about their long-term toxicity. In fact, in most cases, there are limited data about the nanoparticles long-term fate in the body, biodistribution, and safety. Moreover, the optimization of nanomaterials' size to achieve a high tumor accumulation has been the focus of researchers. Nevertheless, recent studies point out that the optimization of the nanomaterials' blood circulation time should be pursued to enhance their tumor accumulation. Additionally, researchers are also starting to consider a step-back on the systemic delivery of anticancer nanomedicines and reexploring the local administration of these antitumoral agents using macroscale delivery platforms (e.g., nanoparticles loaded on microneedles and hydrogels) as tools to improve the therapeutic outcome. These paradigm changes can also explain the slow translation of these materials to the clinic.

Overall, the development of scalable methods for nanomaterials' synthesis, the optimization of their physicochemical properties for enhanced tumor-homing capacity, and the establishment of novel modifications that accelerate their excretion or degradation may contribute to the translation of these theragnostic agents from the bench to the bed side.

Acknowledgments

This work was supported by FEDER funds through the POCI−COMPETE 2020−Operational Programme Competitiveness and Internationalization in Axis I−Strengthening research, technological development and innovation (Project POCI-01-0145-FEDER-007491) and National Funds by FCT−Foundation for Science and Technology (Project UID/Multi/00709/2013). The funding from CENTRO-01-0145-FEDER-028989 is also

acknowledged. Duarte de Melo-Diogo acknowledges CENTRO-01-0145-FEDER-028989 for the funding given on the form of a research contract. André F. Moreira acknowledges his Ph.D. fellowship from FCT (No. SFRH/BD/109482/2015). Carolina F. Rodrigues, Cátia G. Alves, and Rita Lima-Sousa acknowledge funding from the grant UBI-Santander/Totta.

References

Abu Lila, A.S., Kiwada, H., Ishida, T., 2013. The accelerated blood clearance (ABC) phenomenon: clinical challenge and approaches to manage. J. Control. Release 172 (1), 38–47.

Akhtar, M.J., Ahamed, M., Alhadlaq, H.A., Alrokayan, S.A., Kumar, S., 2014. Targeted anticancer therapy: overexpressed receptors and nanotechnology. Clin. Chim. Acta 436, 78–92.

Akhter, S., Ahmad, M.Z., Ahmad, F.J., Storm, G., Kok, R.J., 2012. Gold nanoparticles in theranostic oncology: current state-of-the-art. Expert Opin. Drug Deliv. 9 (10), 1225–1243.

Alex, S., Tiwari, A., 2015. Functionalized gold nanoparticles: synthesis, properties and applications—a review. J. Nanosci. Nanotechnol. 15 (3), 1869–1894.

An, J., Yang, X.-Q., Cheng, K., Song, X.-L., Zhang, L., Li, C., et al., 2017. In vivo computed tomography/photoacoustic imaging and NIR-triggered chemo–photothermal combined therapy based on a gold nanostar-, mesoporous silica-, and thermosensitive liposome-composited nanoprobe. ACS Appl. Mater. Interfaces 9 (48), 41748–41759.

Arnida, Janát-Amsbury, M.M., Ray, A., Peterson, C.M., Ghandehari, H., 2011. Geometry and surface characteristics of gold nanoparticles influence their biodistribution and uptake by macrophages. Eur. J. Pharm. Biopharm. 77 (3), 417–423.

Aryal, S., Grailer, J.J., Pilla, S., Steeber, D.A., Gong, S., 2009. Doxorubicin conjugated gold nanoparticles as water-soluble and pH-responsive anticancer drug nanocarriers. J. Mater. Chem. 19 (42), 7879–7884.

Bao, H., Pan, Y., Ping, Y., Sahoo, N.G., Wu, T., Li, L., et al., 2011. Chitosan-functionalized graphene oxide as a nanocarrier for drug and gene delivery. Small 7 (11), 1569–1578.

Barker, H.E., Paget, J.T.E., Khan, A.A., Harrington, K.J., 2015. The tumour microenvironment after radiotherapy: mechanisms of resistance and recurrence. Nat. Rev. Cancer 15 (7), 409.

Bayda, S., Hadla, M., Palazzolo, S., Riello, P., Corona, G., Toffoli, G., et al., 2018. Inorganic nanoparticles for cancer therapy: a transition from lab to clinic. Curr. Med. Chem. 25 (34), 4269–4303.

Bertrand, N., Grenier, P., Mahmoudi, M., Lima, E.M., Appel, E.A., Dormont, F., et al., 2017. Mechanistic understanding of in vivo protein corona formation on polymeric nanoparticles and impact on pharmacokinetics. Nat. Commun. 8 (1), 777.

Bharti, C., Nagaich, U., Pal, A.K., Gulati, N., 2015. Mesoporous silica nanoparticles in target drug delivery system: a review. Int. J. Pharm. Investig. 5 (3), 124–133.

Black, K.C.L., Wang, Y., Luehmann, H.P., Cai, X., Xing, W., Pang, B., et al., 2014. Radioactive 198Au-doped nanostructures with different shapes for in vivo analyses of their biodistribution, tumor uptake, and intratumoral distribution. ACS Nano 8 (5), 4385–4394.

Blanco, E., Shen, H., Ferrari, M., 2015. Principles of nanoparticle design for overcoming biological barriers to drug delivery. Nat. Biotechnol. 33 (9), 941–951.

Bray, F., Ferlay, J., Soerjomataram, I., Siegel, R.L., Torre, L.A., Jemal, A., 2018. Global cancer statistics 2018: GLOBOCAN estimates of incidence and mortality worldwide for 36 cancers in 185 countries. CA Cancer J. Clin. 68 (6), 394–424.

Champion, J.A., Mitragotri, S., 2006. Role of target geometry in phagocytosis. Proc. Natl. Acad. Sci. U.S.A. 103 (13), 4930.

Chandra, K., Culver, K.S., Werner, S.E., Lee, R.C., Odom, T.W., 2016. Manipulating the anisotropic structure of gold nanostars using good's buffers. Chem. Mater. 28 (18), 6763–6769.

Charnay, C., Bégu, S., Tourné-Péteilh, C., Nicole, L., Lerner, D.A., Devoisselle, J.M., 2004. Inclusion of ibuprofen in mesoporous templated silica: drug loading and release property. Eur. J. Pharm. Biopharm. 57 (3), 533–540.

Chegel, V., Rachkov, O., Lopatynskyi, A., Ishihara, S., Yanchuk, I., Nemoto, Y., et al., 2012. Gold nanoparticles aggregation: drastic effect of cooperative functionalities in a single molecular conjugate. J. Phys. Chem. C 116 (4), 2683–2690.

Chen, J., Wang, D., Xi, J., Au, L., Siekkinen, A., Warsen, A., et al., 2007. Immuno gold nanocages with tailored optical properties for targeted photothermal destruction of cancer cells. Nano Lett. 7 (5), 1318–1322.
Chen, Y.-S., Frey, W., Kim, S., Homan, K., Kruizinga, P., Sokolov, K., et al., 2010. Enhanced thermal stability of silica-coated gold nanorods for photoacoustic imaging and image-guided therapy. Opt. Express 18 (9), 8867–8878.
Chen, B., Liu, M., Zhang, L., Huang, J., Yao, J., Zhang, Z., 2011. Polyethylenimine-functionalized graphene oxide as an efficient gene delivery vector. J. Mater. Chem. 21 (21), 7736–7741.
Chen, D., Feng, H., Li, J., 2012. Graphene oxide: preparation, functionalization, and electrochemical applications. Chem. Rev. 112 (11), 6027–6053.
Chen, J., Zhang, R., Han, L., Tu, B., Zhao, D., 2013. One-pot synthesis of thermally stable gold@ mesoporous silica core-shell nanospheres with catalytic activity. Nano Res. 6 (12), 871–879.
Chen, X., Cheng, X., Soeriyadi, A.H., Sagnella, S.M., Lu, X., Scott, J.A., et al., 2014. Stimuli-responsive functionalized mesoporous silica nanoparticles for drug release in response to various biological stimuli. Biomater. Sci. 2 (1), 121–130.
Cheng, L., Wang, C., Feng, L., Yang, K., Liu, Z., 2014. Functional nanomaterials for phototherapies of cancer. Chem. Rev. 114 (21), 10869–10939.
Cheng, X., Sun, R., Yin, L., Chai, Z., Shi, H., Gao, M., 2017. Light-triggered assembly of gold nanoparticles for photothermal therapy and photoacoustic imaging of tumors in vivo. Adv. Mater. 29 (6), 1604894.
Chien, Y.-H., Chou, Y.-L., Wang, S.-W., Hung, S.-T., Liau, M.-C., Chao, Y.-J., et al., 2013. Near-infrared light photocontrolled targeting, bioimaging, and chemotherapy with caged upconversion nanoparticles in vitro and in vivo. ACS Nano 7 (10), 8516–8528.
Choi, J.D., Lee, J.-S., 2013. Interplay between epigenetics and genetics in cancer. Genomics Inform. 11 (4), 164–173.
Chu, K.F., Dupuy, D.E., 2014. Thermal ablation of tumours: biological mechanisms and advances in therapy. Nat. Rev. Cancer 14 (3), 199–208.
Cole, L.E., Ross, R.D., Tilley, J.M., Vargo-Gogola, T., Roeder, R.K., 2015. Gold nanoparticles as contrast agents in x-ray imaging and computed tomography. Nanomedicine 10 (2), 321–341.
De Melo-Diogo, D., Pais-Silva, C., Costa, E.C., Louro, R.O., Correia, I.J., 2017a. D-α-tocopheryl polyethylene glycol 1000 succinate functionalized nanographene oxide for cancer therapy. Nanomedicine (Lond.) 12 (5), 443–456.
De Melo-Diogo, D., Pais-Silva, C., Dias, D.R., Moreira, A.F., Correia, I.J., 2017b. Strategies to improve cancer photothermal therapy mediated by nanomaterials. Adv. Healthc. Mater. 6 (10).
De Melo-Diogo, D., Costa, E.C., Alves, C.G., Lima-Sousa, R., Ferreira, P., Louro, R.O., et al., 2018a. POxylated graphene oxide nanomaterials for combination chemo-phototherapy of breast cancer cells. Eur. J. Pharm. Biopharm. 131, 162–169.
De Melo-Diogo, D., Lima-Sousa, R., Alves, C.G., Costa, E.C., Louro, R.O., Correia, I.J., 2018b. Functionalization of graphene family nanomaterials for application in cancer therapy. Colloid Surf. B Biointerfaces 171, 260–275.
Dembereldorj, U., Choi, S.Y., Ganbold, E.O., Song, N.W., Kim, D., Choo, J., et al., 2014. Gold nanorod-assembled PEGylated graphene-oxide nanocomposites for photothermal cancer therapy. Photochem. Photobiol. 90 (3), 659–666.
Deng, W., Qiu, J., Wang, S., Yuan, Z., Jia, Y., Tan, H., et al., 2018. Development of biocompatible and VEGF-targeted paclitaxel nanodrugs on albumin and graphene oxide dual-carrier for photothermal-triggered drug delivery in vitro and in vivo. Int. J. Nanomed. 13, 439–453.
Desantis, C.E., Lin, C.C., Mariotto, A.B., Siegel, R.L., Stein, K.D., Kramer, J.L., et al., 2014. Cancer treatment and survivorship statistics, 2014. CA Cancer J. Clin. 64 (4), 252–271.
Dias, D.R., Moreira, A.F., Correia, I.J., 2016. The effect of the shape of gold core–mesoporous silica shell nanoparticles on the cellular behavior and tumor spheroid penetration. J. Mater. Chem. B 4 (47), 7630–7640.
Ding, Y., Zhou, Y.-Y., Chen, H., Geng, D.-D., Wu, D.-Y., Hong, J., et al., 2013. The performance of thiol-terminated PEG-paclitaxel-conjugated gold nanoparticles. Biomaterials 34 (38), 10217–10227.
Dos Santos, M.S.C., Gouvêa, A.L., De Moura, L.D., Paterno, L.G., De Souza, P.E.N., Bastos, A.P., et al., 2018. Nanographene oxide-methylene blue as phototherapies platform for breast tumor ablation and metastasis prevention in a syngeneic orthotopic murine model. J. Nanobiotechnol. 16 (1), 9.
Doshi, N., Prabhakarpandian, B., Rea-Ramsey, A., Pant, K., Sundaram, S., Mitragotri, S., 2010. Flow and adhesion of drug carriers in blood vessels depend on their shape: a study using model synthetic microvascular networks. J. Control. Release 146 (2), 196–200.

Douroumis, D., Onyesom, I., Maniruzzaman, M., Mitchell, J., 2013. Mesoporous silica nanoparticles in nanotechnology. Crit. Rev. Biotechnol. 33 (3), 229–245.
Dreaden, E.C., Alkilany, A.M., Huang, X., Murphy, C.J., El-Sayed, M.A., 2012. The golden age: gold nanoparticles for biomedicine. Chem. Soc. Rev. 41 (7), 2740–2779.
Duan, X., Li, Y., 2013. Physicochemical characteristics of nanoparticles affect circulation, biodistribution, cellular internalization, and trafficking. Small 9 (9–10), 1521–1532.
Eck, W., Craig, G., Sigdel, A., Ritter, G., Old, L.J., Tang, L., et al., 2008. PEGylated gold nanoparticles conjugated to monoclonal F19 antibodies as targeted labeling agents for human pancreatic carcinoma tissue. ACS Nano 2 (11), 2263–2272.
Ernsting, M.J., Murakami, M., Roy, A., Li, S.-D., 2013. Factors controlling the pharmacokinetics, biodistribution and intratumoral penetration of nanoparticles. J. Control. Release 172 (3), 782–794.
Fang, R.H., Kroll, A.V., Gao, W., Zhang, L., 2018. Cell membrane coating nanotechnology. Adv. Mater. 30 (23), 1706759.
Farooq, M.U., Novosad, V., Rozhkova, E.A., Wali, H., Ali, A., Fateh, A.A., et al., 2018. Gold nanoparticles-enabled efficient dual delivery of anticancer therapeutics to HeLa cells. Sci. Rep. 8 (1), 2907.
Feng, L., Yang, X., Shi, X., Tan, X., Peng, R., Wang, J., et al., 2013. Polyethylene glycol and polyethylenimine dual-functionalized nano-graphene oxide for photothermally enhanced gene delivery. Small 9 (11), 1989–1997.
Feng, L., Li, K., Shi, X., Gao, M., Liu, J., Liu, Z., 2014. Smart pH-responsive nanocarriers based on nano-graphene oxide for combined chemo- and photothermal therapy overcoming drug resistance. Adv. Healthc. Mater. 3 (8), 1261–1271.
Foroozandeh, P., Aziz, A.A., 2018. Insight into cellular uptake and intracellular trafficking of nanoparticles. Nanoscale Res. Lett. 13 (1), 339.
Gao, J., Huang, X., Liu, H., Zan, F., Ren, J., 2012. Colloidal stability of gold nanoparticles modified with thiol compounds: bioconjugation and application in cancer cell imaging. Langmuir 28 (9), 4464–4471.
Gao, W., Hu, C.M.J., Fang, R.H., Luk, B.T., Su, J., Zhang, L., 2013. Surface functionalization of gold nanoparticles with red blood cell membranes. Adv. Mater. 25 (26), 3549–3553.
Gessner, A., Lieske, A., Paulke, B.R., Müller, R.H., 2002. Influence of surface charge density on protein adsorption on polymeric nanoparticles: analysis by two-dimensional electrophoresis. Eur. J. Pharm. Biopharm. 54 (2), 165–170.
Ghosh Chaudhuri, R., Paria, S., 2011. Core/shell nanoparticles: classes, properties, synthesis mechanisms, characterization, and applications. Chem. Rev. 112 (4), 2373–2433.
Grün, M., Lauer, I., Unger, K.K., 1997. The synthesis of micrometer- and submicrometer-size spheres of ordered mesoporous oxide MCM-41. Adv. Mater. 9 (3), 254–257.
Guan, X., 2015. Cancer metastases: challenges and opportunities. Acta Pharm. Sin. B 5 (5), 402–418.
Guerrini, L., Alvarez-Puebla, R., Pazos-Perez, N., 2018. Surface modifications of nanoparticles for stability in biological fluids. Materials 11 (7), 1154.
Hanahan, D., Weinberg, R.A., 2011. Hallmarks of cancer: the next generation. Cell 144 (5), 646–674.
Hobbs, S.K., Monsky, W.L., Yuan, F., Roberts, W.G., Griffith, L., Torchilin, V.P., et al., 1998. Regulation of transport pathways in tumor vessels: role of tumor type and microenvironment. Proc. Natl. Acad. Sci. U.S.A. 95 (8), 4607.
Hoshyar, N., Gray, S., Han, H., Bao, G., 2016. The effect of nanoparticle size on in vivo pharmacokinetics and cellular interaction. Nanomedicine 11 (6), 673–692.
Hu, F., Zhang, Y., Chen, G., Li, C., Wang, Q., 2015. Double-walled Au nanocage/SiO_2 nanorattles: integrating SERS imaging, drug delivery and photothermal therapy. Small 11 (8), 985–993.
Hu, Y., He, L., Ma, W., Chen, L., 2018. Reduced graphene oxide-based bortezomib delivery system for photothermal chemotherapy with enhanced therapeutic efficacy. Polym. Int. 67 (12), 1648–1654.
Huang, X., El-Sayed, M.A., 2010. Gold nanoparticles: optical properties and implementations in cancer diagnosis and photothermal therapy. J. Adv. Res. 1 (1), 13–28.
Huang, X., Jain, P.K., El-Sayed, I.H., El-Sayed, M.A., 2007. Gold nanoparticles: interesting optical properties and recent applications in cancer diagnostics and therapy. Nanomedicine (Lond.) 2 (5), 681–693.
Huang, X., Teng, X., Chen, D., Tang, F., He, J., 2010. The effect of the shape of mesoporous silica nanoparticles on cellular uptake and cell function. Biomaterials 31 (3), 438–448.
Huang, H.-C., Barua, S., Sharma, G., Dey, S.K., Rege, K., 2011. Inorganic nanoparticles for cancer imaging and therapy. J. Control. Release 155 (3), 344–357.

Ishida, T., Maeda, R., Ichihara, M., Irimura, K., Kiwada, H., 2003. Accelerated clearance of PEGylated liposomes in rats after repeated injections. J. Control. Release 88 (1), 35–42.
Jain, S., Hirst, D., O'sullivan, J., 2012. Gold nanoparticles as novel agents for cancer therapy. Br. J. Radiol. 85 (1010), 101–113.
Jang, C., Lee, J.H., Sahu, A., Tae, G., 2015. The synergistic effect of folate and RGD dual ligand of nanographene oxide on tumor targeting and photothermal therapy in vivo. Nanoscale 7 (44), 18584–18594.
Kanehara, M., Watanabe, Y., Teranishi, T., 2009. Thermally stable silica-coated hydrophobic gold nanoparticles. J. Nanosci. Nanotechnol. 9 (1), 673–675.
Kang, B., Mackey, M.A., El-Sayed, M.A., 2010. Nuclear targeting of gold nanoparticles in cancer cells induces DNA damage, causing cytokinesis arrest and apoptosis. J. Am. Chem. Soc. 132 (5), 1517–1519.
Kang, S., Lee, J., Ryu, S., Kwon, Y., Kim, K.-H., Jeong, D.H., et al., 2017. Gold nanoparticle/graphene oxide hybrid sheets attached on mesenchymal stem cells for effective photothermal cancer therapy. Chem. Mater. 29 (8), 3461–3476.
Kesse, S., Boakye-Yiadom, K.O., Ochete, B.O., Opoku-Damoah, Y., Akhtar, F., Filli, M.S., et al., 2019. Mesoporous silica nanomaterials: versatile nanocarriers for cancer theranostics and drug and gene delivery. Pharmaceutics 11 (2), 77.
Khalil, I., Julkapli, N., Yehye, W., Basirun, W., Bhargava, S., 2016. Graphene–gold nanoparticles hybrid—synthesis, functionalization, and application in a electrochemical and surface-enhanced Raman scattering biosensor. Materials 9 (6), 406.
Kharazian, B., Hadipour, N.L., Ejtehadi, M.R., 2016. Understanding the nanoparticle–protein corona complexes using computational and experimental methods. Int. J. Biochem. Cell Biol. 75, 162–174.
Kim, Y.K., Na, H.K., Kim, S., Jang, H., Chang, S.J., Min, D.H., 2015. One-pot synthesis of multifunctional Au@graphene oxide nanocolloid core@shell nanoparticles for Raman bioimaging, photothermal, and photodynamic therapy. Small 11 (21), 2527–2535.
Knop, K., Hoogenboom, R., Fischer, D., Schubert, U.S., 2010. Poly(ethylene glycol) in drug delivery: pros and cons as well as potential alternatives. Angew. Chem. Int. Ed. 49 (36), 6288–6308.
Kobayashi, Y., Correa-Duarte, M.A., Liz-Marzán, L.M., 2001. Sol − gel processing of silica-coated gold nanoparticles. Langmuir 17 (20), 6375–6379.
Kobayashi, Y., Inose, H., Nakagawa, T., Kubota, Y., Gonda, K., Ohuchi, N., 2013. X-ray imaging technique using colloid solution of Au/silica core-shell nanoparticles. J. Nanostruct. Chem. 3 (1), 62.
Kolate, A., Baradia, D., Patil, S., Vhora, I., Kore, G., Misra, A., 2014. PEG—a versatile conjugating ligand for drugs and drug delivery systems. J. Control. Release 192, 67–81.
Kundu, S., Lau, S., Liang, H., 2009. Shape-controlled catalysis by cetyltrimethylammonium bromide terminated gold nanospheres, nanorods, and nanoprisms. J. Phys. Chem. C 113 (13), 5150–5156.
Lee, Y.K., Choi, E.-J., Webster, T.J., Kim, S.-H., Khang, D., 2014. Effect of the protein corona on nanoparticles for modulating cytotoxicity and immunotoxicity. Int. J. Nanomed. 10, 97–113.
Lee, J.H., Sahu, A., Jang, C., Tae, G., 2015. The effect of ligand density on in vivo tumor targeting of nanographene oxide. J. Control. Release 209, 219–228.
Li, W., Chen, X., 2015. Gold nanoparticles for photoacoustic imaging. Nanomedicine 10 (2), 299–320.
Li, Z., Barnes, J.C., Bosoy, A., Stoddart, J.F., Zink, J.I., 2012. Mesoporous silica nanoparticles in biomedical applications. Chem. Soc. Rev. 41 (7), 2590–2605.
Li, N., Zhao, P., Astruc, D., 2014a. Anisotropic gold nanoparticles: synthesis, properties, applications, and toxicity. Angew. Chem. Int. Ed. 53 (7), 1756–1789.
Li, Y., Feng, L., Shi, X., Wang, X., Yang, Y., Yang, K., et al., 2014b. Surface coating-dependent cytotoxicity and degradation of graphene derivatives: towards the design of non-toxic, degradable nano-graphene. Small 10 (8), 1544–1554.
Li, X., Wu, M., Pan, L., Shi, J., 2015a. Tumor vascular-targeted co-delivery of anti-angiogenesis and chemotherapeutic agents by mesoporous silica nanoparticle-based drug delivery system for synergetic therapy of tumor. Int. J. Nanomed. 11, 93–105.
Li, Z.-Y., Hu, J.-J., Xu, Q., Chen, S., Jia, H.-Z., Sun, Y.-X., et al., 2015b. A redox-responsive drug delivery system based on RGD containing peptide-capped mesoporous silica nanoparticles. J. Mater. Chem. B 3 (1), 39–44.
Li, H.-J., Du, J.-Z., Du, X.-J., Xu, C.-F., Sun, C.-Y., Wang, H.-X., et al., 2016. Stimuli-responsive clustered nanoparticles for improved tumor penetration and therapeutic efficacy. Proc. Natl. Acad. Sci. U.S.A. 113 (15), 4164.

Li, X., Hu, Z., Ma, J., Wang, X., Zhang, Y., Wang, W., et al., 2018. The systematic evaluation of size-dependent toxicity and multi-time biodistribution of gold nanoparticles. Colloid Surf. B Biointerfaces 167, 260–266.
Lima-Sousa, R., De Melo-Diogo, D., Alves, C.G., Costa, E.C., Ferreira, P., Louro, R.O., et al., 2018. Hyaluronic acid functionalized green reduced graphene oxide for targeted cancer photothermal therapy. Carbohydr. Polym. 200, 93–99.
Lin, G., Mi, P., Chu, C., Zhang, J., Liu, G., 2016. Inorganic nanocarriers overcoming multidrug resistance for cancer theranostics. Adv. Sci. 3 (11), 1600134.
Lin, J., Huang, Y., Huang, P., 2018. Chapter 9: Graphene-based nanomaterials in bioimaging. In: Sarmento, B., Das Neves, J. (Eds.), Biomedical Applications of Functionalized Nanomaterials. Elsevier.
Liu, J., Peng, Q., 2017. Protein-gold nanoparticle interactions and their possible impact on biomedical applications. Acta Biomater. 55, 13–27.
Liu, Z., Robinson, J.T., Sun, X., Dai, H., 2008. PEGylated nanographene oxide for delivery of water-insoluble cancer drugs. J. Am. Chem. Soc. 130 (33), 10876–10877.
Liu, X., Tao, H., Yang, K., Zhang, S., Lee, S.-T., Liu, Z., 2011. Optimization of surface chemistry on single-walled carbon nanotubes for in vivo photothermal ablation of tumors. Biomaterials 32 (1), 144–151.
Liu, J., Cui, L., Losic, D., 2013. Graphene and graphene oxide as new nanocarriers for drug delivery applications. Acta Biomater. 9 (12), 9243–9257.
Liu, H., Doane, T.L., Cheng, Y., Lu, F., Srinivasan, S., Zhu, J.-J., et al., 2015a. Control of surface ligand density on PEGylated gold nanoparticles for optimized cancer cell uptake. Part. Part. Syst. Charact. 32 (2), 197–204.
Liu, J., Detrembleur, C., De Pauw-Gillet, M.C., Mornet, S., Jérôme, C., Duguet, E., 2015b. Gold nanorods coated with mesoporous silica shell as drug delivery system for remote near infrared light-activated release and potential phototherapy. Small 11 (19), 2323–2332.
Liu, Y., Ashton, J.R., Moding, E.J., Yuan, H., Register, J.K., Fales, A.M., et al., 2015c. A plasmonic gold nanostar theranostic probe for in vivo tumor imaging and photothermal therapy. Theranostics 5 (9), 946–960.
Liu, C.-C., Zhao, J.-J., Zhang, R., Li, H., Chen, B., Zhang, L.-L., et al., 2017. Multifunctionalization of graphene and graphene oxide for controlled release and targeted delivery of anticancer drugs. Am. J. Transl. Res. 9 (12), 5197.
Liu, R., Zhang, H., Zhang, F., Wang, X., Liu, X., Zhang, Y., 2019. Polydopamine doped reduced graphene oxide/mesoporous silica nanosheets for chemo-photothermal and enhanced photothermal therapy. Mater. Sci. Eng. C. 96, 138–145.
Lohse, S.E., Murphy, C.J., 2013. The quest for shape control: a history of gold nanorod synthesis. Chem. Mater. 25 (8), 1250–1261.
Love, J.C., Estroff, L.A., Kriebel, J.K., Nuzzo, R.G., Whitesides, G.M., 2005. Self-assembled monolayers of thiolates on metals as a form of nanotechnology. Chem. Rev. 105 (4), 1103–1170.
Luo, G.F., Chen, W.H., Lei, Q., Qiu, W.X., Liu, Y.X., Cheng, Y.J., et al., 2016a. A triple-collaborative strategy for high-performance tumor therapy by multifunctional mesoporous silica-coated gold nanorods. Adv. Funct. Mater. 26 (24), 4339–4350.
Luo, S., Yang, Z., Tan, X., Wang, Y., Zeng, Y., Wang, Y., et al., 2016b. Multifunctional photosensitizer grafted on polyethylene glycol and polyethylenimine dual-functionalized nanographene oxide for cancer-targeted near-infrared imaging and synergistic phototherapy. ACS Appl. Mater. Interfaces 8 (27), 17176–17186.
Mackey, M.A., Ali, M.R., Austin, L.A., Near, R.D., El-Sayed, M.A., 2014. The most effective gold nanorod size for plasmonic photothermal therapy: theory and in vitro experiments. J. Phys. Chem. B 118 (5), 1319–1326.
Mamaeva, V., Sahlgren, C., Lindén, M., 2013. Mesoporous silica nanoparticles in medicine—recent advances. Adv. Drug Deliv. Rev. 65 (5), 689–702.
Marcano, D.C., Kosynkin, D.V., Berlin, J.M., Sinitskii, A., Sun, Z., Slesarev, A., et al., 2010. Improved synthesis of graphene oxide. ACS Nano 4 (8), 4806–4814.
Matsumoto, Y., Nichols, J.W., Toh, K., Nomoto, T., Cabral, H., Miura, Y., et al., 2016. Vascular bursts enhance permeability of tumour blood vessels and improve nanoparticle delivery. Nat. Nanotechnol. 11, 533.
Meng, H., Mai, W.X., Zhang, H., Xue, M., Xia, T., Lin, S., et al., 2013. Codelivery of an optimal drug/siRNA combination using mesoporous silica nanoparticles to overcome drug resistance in breast cancer in vitro and in vivo. ACS Nano 7 (2), 994–1005.
Mine, E., Yamada, A., Kobayashi, Y., Konno, M., Liz-Marzán, L.M., 2003. Direct coating of gold nanoparticles with silica by a seeded polymerization technique. J. Colloid Interface Sci. 264 (2), 385–390.

Mirza, A.Z., Shamshad, H., 2011. Preparation and characterization of doxorubicin functionalized gold nanoparticles. Eur. J. Med. Chem. 46 (5), 1857–1860.
Mitragotri, S., Burke, P.A., Langer, R., 2014. Overcoming the challenges in administering biopharmaceuticals: formulation and delivery strategies. Nat. Rev. Drug Discov. 13, 655.
Moreira, A.F., Gaspar, V.M., Costa, E.C., De Melo-Diogo, D., Machado, P., Paquete, C.M., et al., 2014. Preparation of end-capped pH-sensitive mesoporous silica nanocarriers for on-demand drug delivery. Eur. J. Pharm. Biopharm. 88 (3), 1012–1025.
Moreira, A.F., Dias, D.R., Correia, I.J., 2016. Stimuli-responsive mesoporous silica nanoparticles for cancer therapy: a review. Micropor. Mesopor. Mater. 236, 141–157.
Moreira, A.F., Rodrigues, C.F., Reis, C.A., Costa, E.C., Correia, I.J., 2018a. Gold-core silica shell nanoparticles application in imaging and therapy: a review. Micropor. Mesopor. Mater. 270, 168–179.
Moreira, A.F., Rodrigues, C.F., Reis, C.A., Costa, E.C., Ferreira, P., Correia, I.J., 2018b. Development of poly-2-ethyl-2-oxazoline coated gold-core silica shell nanorods for cancer chemo-photothermal therapy. Nanomedicine 13 (20), 2611–2627.
Mura, S., Nicolas, J., Couvreur, P., 2013. Stimuli-responsive nanocarriers for drug delivery. Nat. Mater. 12, 991–1003.
Nergiz, S.Z., Gandra, N., Tadepalli, S., Singamaneni, S., 2014. Multifunctional hybrid nanopatches of graphene oxide and gold nanostars for ultraefficient photothermal cancer therapy. ACS Appl. Mater. Interfaces 6 (18), 16395–16402.
Niedermayer, S., Weiss, V., Herrmann, A., Schmidt, A., Datz, S., Müller, K., et al., 2015. Multifunctional polymer-capped mesoporous silica nanoparticles for pH-responsive targeted drug delivery. Nanoscale 7 (17), 7953–7964.
Otsuka, H., Nagasaki, Y., Kataoka, K., 2012. PEGylated nanoparticles for biological and pharmaceutical applications. Adv. Drug Deliv. Rev. 64, 246–255.
Patel, S.C., Lee, S., Lalwani, G., Suhrland, C., Chowdhury, S.M., Sitharaman, B., 2016. Graphene-based platforms for cancer therapeutics. Ther. Deliv. 7 (2), 101–116.
Pei, S., Cheng, H.-M., 2012. The reduction of graphene oxide. Carbon 50 (9), 3210–3228.
Peiris, P.M., Deb, P., Doolittle, E., Doron, G., Goldberg, A., Govender, P., et al., 2015. Vascular targeting of a gold nanoparticle to breast cancer metastasis. J. Pharm. Sci. 104 (8), 2600–2610.
Perrault, S.D., Walkey, C., Jennings, T., Fischer, H.C., Chan, W.C.W., 2009. Mediating tumor targeting efficiency of nanoparticles through design. Nano Lett. 9 (5), 1909–1915.
Pozzi, D., Colapicchioni, V., Caracciolo, G., Piovesana, S., Capriotti, A.L., Palchetti, S., et al., 2014. Effect of polyethyleneglycol (PEG) chain length on the bio–nano-interactions between PEGylated lipid nanoparticles and biological fluids: from nanostructure to uptake in cancer cells. Nanoscale 6 (5), 2782–2792.
Qian, J., Wang, D., Cai, F., Zhan, Q., Wang, Y., He, S., 2012. Photosensitizer encapsulated organically modified silica nanoparticles for direct two-photon photodynamic therapy and in vivo functional imaging. Biomaterials 33 (19), 4851–4860.
Qin, X.C., Guo, Z.Y., Liu, Z.M., Zhang, W., Wan, M.M., Yang, B.W., 2013. Folic acid-conjugated graphene oxide for cancer targeted chemo-photothermal therapy. J. Photochem. Photobiol. B Biol. 120, 156–162.
Qiu, Y., Liu, Y., Wang, L., Xu, L., Bai, R., Ji, Y., et al., 2010. Surface chemistry and aspect ratio mediated cellular uptake of Au nanorods. Biomaterials 31 (30), 7606–7619.
Reis, C.A., Rodrigues, C.F., Moreira, A.F., Jacinto, T.A., Ferreira, P., Correia, I.J., 2019. Development of gold-core silica shell nanospheres coated with poly-2-ethyl-oxazoline and β-cyclodextrin aimed for cancer therapy. Mater. Sci. Eng. C 98, 960–968.
Reuveni, T., Motiei, M., Romman, Z., Popovtzer, A., Popovtzer, R., 2011. Targeted gold nanoparticles enable molecular CT imaging of cancer: an in vivo study. Int. J. Nanomed. 6, 2859.
Robinson, J.T., Tabakman, S.M., Liang, Y., Wang, H., Sanchez Casalongue, H., Vinh, D., et al., 2011. Ultrasmall reduced graphene oxide with high near-infrared absorbance for photothermal therapy. J. Am. Chem. Soc. 133 (17), 6825–6831.
Rodrigues, C.F., Jacinto, T.A., Moreira, A.F., Costa, E.C., Miguel, S.P., Correia, I.J., 2019a. Functionalization of AuMSS nanorods towards more effective cancer therapies. Nano Res. 12 (4), 1–14.
Rodrigues, C.F., Reis, C.A., Moreira, A.F., Ferreira, P., Correia, I.J., 2019b. Optimization of gold core-mesoporous silica shell functionalization with TPGS and PEI for cancer therapy. Micropor. Mesopor. Mater. 285, 1–12.

Ruan, S., Cao, X., Cun, X., Hu, G., Zhou, Y., Zhang, Y., et al., 2015. Matrix metalloproteinase-sensitive size-shrinkable nanoparticles for deep tumor penetration and pH triggered doxorubicin release. Biomaterials 60, 100–110.
Sahu, A., Choi, W.I., Lee, J.H., Tae, G., 2013. Graphene oxide mediated delivery of methylene blue for combined photodynamic and photothermal therapy. Biomaterials 34 (26), 6239–6248.
Salvati, A., Pitek, A.S., Monopoli, M.P., Prapainop, K., Bombelli, F.B., Hristov, D.R., et al., 2013. Transferrin-functionalized nanoparticles lose their targeting capabilities when a biomolecule corona adsorbs on the surface. Nat. Nanotechnol. 8, 137.
Saw, W.S., Ujihara, M., Chong, W.Y., Voon, S.H., Imae, T., Kiew, L.V., et al., 2018. Size-dependent effect of cystine/citric acid-capped confeito-like gold nanoparticles on cellular uptake and photothermal cancer therapy. Colloid Surf. B: Biointerfaces 161, 365–374.
Seo, S.-H., Kim, B.-M., Joe, A., Han, H.-W., Chen, X., Cheng, Z., et al., 2014. NIR-light-induced surface-enhanced Raman scattering for detection and photothermal/photodynamic therapy of cancer cells using methylene blue-embedded gold nanorod@SiO_2 nanocomposites. Biomaterials 35 (10), 3309–3318.
Shao, L., Zhang, R., Lu, J., Zhao, C., Deng, X., Wu, Y., 2017. Mesoporous silica coated polydopamine functionalized reduced graphene oxide for synergistic targeted chemo-photothermal therapy. ACS Appl. Mater. Interfaces 9 (2), 1226–1236.
Shi, S., Yang, K., Hong, H., Valdovinos, H.F., Nayak, T.R., Zhang, Y., et al., 2013a. Tumor vasculature targeting and imaging in living mice with reduced graphene oxide. Biomaterials 34 (12), 3002–3009.
Shi, X., Gong, H., Li, Y., Wang, C., Cheng, L., Liu, Z., 2013b. Graphene-based magnetic plasmonic nanocomposite for dual bioimaging and photothermal therapy. Biomaterials 34 (20), 4786–4793.
Shim, G., Kim, M.-G., Park, J.Y., Oh, Y.-K., 2016. Graphene-based nanosheets for delivery of chemotherapeutics and biological drugs. Adv. Drug Deliv. Rev. 105, 205–227.
Silva, A.S., Silva, M.C., Miguel, S.P., Bonifácio, V.D.B., Correia, I.J., Aguiar-Ricardo, A., 2016. Nanogold POxylation: towards always-on fluorescent lung cancer targeting. RSC Adv. 6 (40), 33631–33635.
Song, J.-T., Yang, X.-Q., Zhang, X.-S., Yan, D.-M., Wang, Z.-Y., Zhao, Y.-D., 2015. Facile synthesis of gold nanospheres modified by positively charged mesoporous silica, loaded with near-infrared fluorescent dye, for in vivo X-ray computed tomography and fluorescence dual mode imaging. ACS Appl. Mater. Interfaces 7 (31), 17287–17297.
Stöber, W., Fink, A., Bohn, E., 1968. Controlled growth of monodisperse silica spheres in the micron size range. J. Colloid Interface Sci. 26 (1), 62–69.
Stuchinskaya, T., Moreno, M., Cook, M.J., Edwards, D.R., Russell, D.A., 2011. Targeted photodynamic therapy of breast cancer cells using antibody–phthalocyanine–gold nanoparticle conjugates. Photochem. Photobiol. Sci. 10 (5), 822–831.
Sun, S., Wu, P., 2011. Competitive surface-enhanced Raman scattering effects in noble metal nanoparticle-decorated graphene sheets. Phys. Chem. Chem. Phys. 13 (47), 21116–21120.
Sun, B., Wu, J., Cui, S., Zhu, H., An, W., Fu, Q., et al., 2017a. In situ synthesis of graphene oxide/gold nanorods theranostic hybrids for efficient tumor computed tomography imaging and photothermal therapy. Nano Res. 10 (1), 37–48.
Sun, H., Su, J., Meng, Q., Yin, Q., Chen, L., Gu, W., et al., 2017b. Cancer cell membrane-coated gold nanocages with hyperthermia-triggered drug release and homotypic target inhibit growth and metastasis of breast cancer. Adv. Funct. Mater. 27 (3), 1604300.
Ta, H.T., Truong, N.P., Whittaker, A.K., Davis, T.P., Peter, K., 2018. The effects of particle size, shape, density and flow characteristics on particle margination to vascular walls in cardiovascular diseases. Expert Opin. Drug Deliv. 15 (1), 33–45.
Tang, S., Huang, X., Zheng, N., 2011. Silica coating improves the efficacy of Pd nanosheets for photothermal therapy of cancer cells using near infrared laser. Chem. Commun. 47 (13), 3948–3950.
Tang, Y., Hu, H., Zhang, M.G., Song, J., Nie, L., Wang, S., et al., 2015. An aptamer-targeting photoresponsive drug delivery system using "off–on" graphene oxide wrapped mesoporous silica nanoparticles. Nanoscale 7 (14), 6304–6310.
Tao, Y., Ju, E., Ren, J., Qu, X., 2014. Immunostimulatory oligonucleotides-loaded cationic graphene oxide with photothermally enhanced immunogenicity for photothermal/immune cancer therapy. Biomaterials 35 (37), 9963–9971.

Tian, B., Wang, C., Zhang, S., Feng, L., Liu, Z., 2011. Photothermally enhanced photodynamic therapy delivered by nano-graphene oxide. ACS Nano 5 (9), 7000–7009.
Tian, J., Luo, Y., Huang, L., Feng, Y., Ju, H., Yu, B.-Y., 2016. Pegylated folate and peptide-decorated graphene oxide nanovehicle for in vivo targeted delivery of anticancer drugs and therapeutic self-monitoring. Biosens. Bioelectron. 80, 519–524.
Tong, W., Walsh, M.J., Mulvaney, P., Etheridge, J., Funston, A.M., 2017. Control of symmetry breaking size and aspect ratio in gold nanorods: underlying role of silver nitrate. J. Phys. Chem. C 121 (6), 3549–3559.
Toy, R., Peiris, P.M., Ghaghada, K.B., Karathanasis, E., 2014. Shaping cancer nanomedicine: the effect of particle shape on the in vivo journey of nanoparticles. Nanomedicine 9 (1), 121–134.
Tran, T.H., Nguyen, H.T., Pham, T.T., Choi, J.Y., Choi, H.-G., Yong, C.S., et al., 2015. Development of a graphene oxide nanocarrier for dual-drug chemo-phototherapy to overcome drug resistance in cancer. ACS Appl. Mater. Interfaces 7 (51), 28647–28655.
Tukappa, A., Ultimo, A., De La Torre, C., Pardo, T., Sancenón, F., Martínez-Máñez, R., 2016. Polyglutamic acid-gated mesoporous silica nanoparticles for enzyme-controlled drug delivery. Langmuir 32 (33), 8507–8515.
Uz, M., Bulmus, V., Alsoy Altinkaya, S., 2016. Effect of PEG grafting density and hydrodynamic volume on gold nanoparticle–cell interactions: an investigation on cell cycle, apoptosis, and DNA damage. Langmuir 32 (23), 5997–6009.
Verma, M., Sheoran, P., Chaudhury, A., 2018. Application of nanotechnology for cancer treatment. In: Gahlawat, S.K., Duhan, J.S., Salar, R.K., Siwach, P., Kumar, S., Kaur, P. (Eds.), Advances in Animal Biotechnology and Its Applications. Springer Singapore, Singapore.
Vilalta, M., Rafat, M., Graves, E.E., 2016. Effects of radiation on metastasis and tumor cell migration. Cell. Mol. Life Sci. 73 (16), 2999–3007.
Walkey, C.D., Olsen, J.B., Guo, H., Emili, A., Chan, W.C.W., 2012. Nanoparticle size and surface chemistry determine serum protein adsorption and macrophage uptake. J. Am. Chem. Soc. 134 (4), 2139–2147.
Wan, X., Zhang, J., Yu, W., Shen, L., Ji, S., Hu, T., 2017. Effect of protein immunogenicity and PEG size and branching on the anti-PEG immune response to PEGylated proteins. Process. Biochem. 52, 183–191.
Wang, C., Li, J., Amatore, C., Chen, Y., Jiang, H., Wang, X.M., 2011a. Gold nanoclusters and graphene nanocomposites for drug delivery and imaging of cancer cells. Angew. Chem. Int. Ed. 50 (49), 11644–11648.
Wang, F., Wang, Y.-C., Dou, S., Xiong, M.-H., Sun, T.-M., Wang, J., 2011b. Doxorubicin-tethered responsive gold nanoparticles facilitate intracellular drug delivery for overcoming multidrug resistance in cancer cells. ACS Nano 5 (5), 3679–3692.
Wang, H., Zheng, L., Peng, C., Shen, M., Shi, X., Zhang, G., 2013a. Folic acid-modified dendrimer-entrapped gold nanoparticles as nanoprobes for targeted CT imaging of human lung adencarcinoma. Biomaterials 34 (2), 470–480.
Wang, Y., Black, K.C.L., Luehmann, H., Li, W., Zhang, Y., Cai, X., et al., 2013b. Comparison study of gold nanohexapods, nanorods, and nanocages for photothermal cancer treatment. ACS Nano 7 (3), 2068–2077.
Wang, Y., Wang, K., Zhao, J., Liu, X., Bu, J., Yan, X., et al., 2013c. Multifunctional mesoporous silica-coated graphene nanosheet used for chemo-photothermal synergistic targeted therapy of glioma. J. Am. Chem. Soc. 135 (12), 4799–4804.
Wang, D., Xu, Z., Yu, H., Chen, X., Feng, B., Cui, Z., et al., 2014. Treatment of metastatic breast cancer by combination of chemotherapy and photothermal ablation using doxorubicin-loaded DNA wrapped gold nanorods. Biomaterials 35 (29), 8374–8384.
Wang, J., Bai, R., Yang, R., Liu, J., Tang, J., Liu, Y., et al., 2015a. Size- and surface chemistry-dependent pharmacokinetics and tumor accumulation of engineered gold nanoparticles after intravenous administration. Metallomics 7 (3), 516–524.
Wang, S., Teng, Z., Huang, P., Liu, D., Liu, Y., Tian, Y., et al., 2015b. Reversibly extracellular pH controlled cellular uptake and photothermal therapy by PEGylated mixed-charge gold nanostars. Small 11 (15), 1801–1810.
Wang, Y., Zhao, Q., Han, N., Bai, L., Li, J., Liu, J., et al., 2015c. Mesoporous silica nanoparticles in drug delivery and biomedical applications. Nanomed. Nanotechnol. Biol. Med. 11 (2), 313–327.
Wang, F., Sun, Q., Feng, B., Xu, Z., Zhang, J., Xu, J., et al., 2016. Polydopamine-functionalized graphene oxide loaded with gold nanostars and doxorubicin for combined photothermal and chemotherapy of metastatic breast cancer. Adv. Healthc. Mater. 5 (17), 2227–2236.
Wen, S., Li, K., Cai, H., Chen, Q., Shen, M., Huang, Y., et al., 2013. Multifunctional dendrimer-entrapped gold nanoparticles for dual mode CT/MR imaging applications. Biomaterials 34 (5), 1570–1580.

Woehrle, G.H., Brown, L.O., Hutchison, J.E., 2005. Thiol-functionalized, 1.5-nm gold nanoparticles through ligand exchange reactions: scope and mechanism of ligand exchange. J. Am. Chem. Soc. 127 (7), 2172–2183.
Wrighton, K.H., 2019. Trafficking signals for metastasis. Nat. Rev. Cancer 19 (3), 127.
Wu, S.-H., Mou, C.-Y., Lin, H.-P., 2013. Synthesis of mesoporous silica nanoparticles. Chem. Soc. Rev. 42 (9), 3862–3875.
Wu, S.-Y., An, S.S.A., Hulme, J., 2015. Current applications of graphene oxide in nanomedicine. Int. J. Nanomed. 10 (Spec Iss), 9.
Wu, L., Xie, J., Li, T., Mai, Z., Wang, L., Wang, X., et al., 2017. Gene delivery ability of polyethylenimine and polyethylene glycol dual-functionalized nanographene oxide in 11 different cell lines. R. Soc. Open Sci. 4 (10), 170822.
Xi, D., Dong, S., Meng, X., Lu, Q., Meng, L., Ye, J., 2012. Gold nanoparticles as computerized tomography (CT) contrast agents. RSC Adv. 2 (33), 12515–12524.
Xia, X., Xia, Y., 2014. Gold nanocages as multifunctional materials for nanomedicine. Front. Phys. 9 (3), 378–384.
Xiao, K., Li, Y., Luo, J., Lee, J.S., Xiao, W., Gonik, A.M., et al., 2011. The effect of surface charge on in vivo biodistribution of PEG-oligocholic acid based micellar nanoparticles. Biomaterials 32 (13), 3435–3446.
Xie, X., Liao, J., Shao, X., Li, Q., Lin, Y., 2017. The effect of shape on cellular uptake of gold nanoparticles in the forms of stars, rods, and triangles. Sci. Rep. 7 (1), 3827.
Xu, C., Chen, F., Valdovinos, H.F., Jiang, D., Goel, S., Yu, B., et al., 2018. Bacteria-like mesoporous silica-coated gold nanorods for positron emission tomography and photoacoustic imaging-guided chemo-photothermal combined therapy. Biomaterials 165, 56–65.
Xuan, M., Shao, J., Dai, L., Li, J., He, Q., 2016. Macrophage cell membrane camouflaged Au nanoshells for in vivo prolonged circulation life and enhanced cancer photothermal therapy. ACS Appl. Mater. Interfaces 8 (15), 9610–9618.
Yan, M., Liu, Y., Zhu, X., Wang, X., Liu, L., Sun, H., et al., 2018. Nanoscale reduced graphene oxide-mediated photothermal therapy together with IDO inhibition and PD-L1 blockade synergistically promote antitumor immunity. ACS Appl. Mater. Interfaces 11 (2), 1876–1885.
Yang, K., Zhang, S., Zhang, G., Sun, X., Lee, S.-T., Liu, Z., 2010. Graphene in mice: ultrahigh in vivo tumor uptake and efficient photothermal therapy. Nano Lett. 10 (9), 3318–3323.
Yang, K., Hu, L., Ma, X., Ye, S., Cheng, L., Shi, X., et al., 2012a. Multimodal imaging guided photothermal therapy using functionalized graphene nanosheets anchored with magnetic nanoparticles. Adv. Mater. 24 (14), 1868–1872.
Yang, K., Wan, J., Zhang, S., Tian, B., Zhang, Y., Liu, Z., 2012b. The influence of surface chemistry and size of nanoscale graphene oxide on photothermal therapy of cancer using ultra-low laser power. Biomaterials 33 (7), 2206–2214.
Yang, K., Feng, L., Shi, X., Liu, Z., 2013. Nano-graphene in biomedicine: theranostic applications. Chem. Soc. Rev. 42 (2), 530–547.
Yang, Q., Jones, S.W., Parker, C.L., Zamboni, W.C., Bear, J.E., Lai, S.K., 2014. Evading immune cell uptake and clearance requires PEG grafting at densities substantially exceeding the minimum for brush conformation. Mol. Pharm. 11 (4), 1250–1258.
Yang, X., Yang, M.X., Pang, B., Vara, M., Xia, Y.N., 2015. Gold nanomaterials at work in biomedicine. Chem. Rev. 115 (19), 10410–10488.
Yasun, E., Li, C., Barut, I., Janvier, D., Qiu, L., Cui, C., et al., 2015. BSA modification to reduce CTAB induced non-specificity and cytotoxicity of aptamer-conjugated gold nanorods. Nanoscale 7 (22), 10240–10248.
Yi, L., Zhang, Y., Shi, X., Du, X., Wang, X., Yu, A., et al., 2019. Recent progress of functionalised graphene oxide in cancer therapy. J. Drug Target. 27 (2), 125–144.
Yin, F., Hu, K., Chen, Y., Yu, M., Wang, D., Wang, Q., et al., 2017. SiRNA delivery with PEGylated graphene oxide nanosheets for combined photothermal and genetherapy for pancreatic cancer. Theranostics 7 (5), 1133.
Yue, J., Feliciano, T.J., Li, W., Lee, A., Odom, T.W., 2017. Gold nanoparticle size and shape effects on cellular uptake and intracellular distribution of siRNA nanoconstructs. Bioconjugate Chem. 28 (6), 1791–1800.
Zhang, G., Gao, J., Qian, J., Zhang, L., Zheng, K., Zhong, K., et al., 2015a. Hydroxylated mesoporous nanosilica coated by polyethylenimine coupled with gadolinium and folic acid: a tumor-targeted T1 magnetic resonance contrast agent and drug delivery system. ACS Appl. Mater. Interfaces 7 (26), 14192–14200.

Zhang, T., Ding, Z., Lin, H., Cui, L., Yang, C., Li, X., et al., 2015b. pH-sensitive gold nanorods with a mesoporous silica shell for drug release and photothermal therapy. Eur. J. Inorg. Chem. 2015 (13), 2277–2284.
Zhang, Z., Liu, C., Bai, J., Wu, C., Xiao, Y., Li, Y., et al., 2015c. Silver nanoparticle gated, mesoporous silica coated gold nanorods (AuNR@MS@AgNPs): low premature release and multifunctional cancer theranostic platform. ACS Appl. Mater. Interfaces 7 (11), 6211–6219.
Zhang, W., Shen, J., Su, H., Mu, G., Sun, J.-H., Tan, C.-P., et al., 2016. Co-delivery of cisplatin prodrug and chlorin e6 by mesoporous silica nanoparticles for chemo-photodynamic combination therapy to combat drug resistance. ACS Appl. Mater. Interfaces 8 (21), 13332–13340.
Zhang, D.-Y., Zheng, Y., Tan, C.-P., Sun, J.-H., Zhang, W., Ji, L.-N., et al., 2017. Graphene oxide decorated with Ru (II)–polyethylene glycol complex for lysosome-targeted imaging and photodynamic/photothermal therapy. ACS Appl. Mater. Interfaces 9 (8), 6761–6771.
Zhang, Y., Cai, K., Li, C., Guo, Q., Chen, Q., He, X., et al., 2018. Macrophage-membrane-coated nanoparticles for tumor-targeted chemotherapy. Nano Lett. 18 (3), 1908–1915.
Zhang, Y.-R., Lin, R., Li, H.-J., He, W.-L., Du, J.-Z., Wang, J., 2019. Strategies to improve tumor penetration of nanomedicines through nanoparticle design. Wiley Interdiscip. Rev. Nanomed. Nanobiotechnol. 11 (1), e1519.
Zhao, P., Li, N., Astruc, D., 2013. State of the art in gold nanoparticle synthesis. Coord. Chem. Rev. 257 (3–4), 638–665.
Zhou, H., Xu, H., Li, X., Lv, Y., Ma, T., Guo, S., et al., 2017. Dual targeting hyaluronic acid-RGD mesoporous silica coated gold nanorods for chemo-photothermal cancer therapy. Mater. Sci. Eng. C 81, 261–270.
Zhou, Y., Quan, G., Wu, Q., Zhang, X., Niu, B., Wu, B., et al., 2018. Mesoporous silica nanoparticles for drug and gene delivery. Acta Pharm. Sin. B 8 (2), 165–177.
Zhu, Y., Murali, S., Cai, W., Li, X., Suk, J.W., Potts, J.R., et al., 2010. Graphene and graphene oxide: synthesis, properties, and applications. Adv. Mater. 22 (35), 3906–3924.